# General Disclaimer

## One or more of the Following Statements may affect this Document

- This document has been reproduced from the best copy furnished by the organizational source. It is being released in the interest of making available as much information as possible.

- This document may contain data, which exceeds the sheet parameters. It was furnished in this condition by the organizational source and is the best copy available.

- This document may contain tone-on-tone or color graphs, charts and/or pictures, which have been reproduced in black and white.

- This document is paginated as submitted by the original source.

- Portions of this document are not fully legible due to the historical nature of some of the material. However, it is the best reproduction available from the original submission.

Produced by the NASA Center for Aerospace Information (CASI)

Final Technical Report

NASA Grant NAG 5-136

Atmospheric Planetary Wave Response to External Forcing

Principal Investigator:     Duane E. Stevens

Co-Investigator:            Elmar R. Reiter

Department of Atmospheric Science

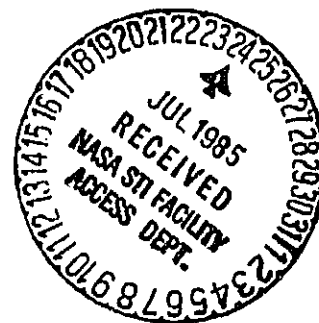Colorado State University

June 1985

# Table of Contents

# 1. Introduction and Overview

This volume contains the Final Technical Report of the research performed at Colorado State University under the auspices of NASA Grant 5-136 entitled "Atmospheric Planetary Wave Response to External Forcing." In this research effort, our intent has been to combine the tools of observational analysis, complex general circulation modeling, and simpler modeling approaches in order to attack problems on the largest spatial scales of the earth's atmosphere.

Most of our energies have been expended in the development and application of two different models. The first is a two-level, global spectral model which was designed primarily to test the effects of north-south sea surface temperature anomaly (SSTA) gradients between the equatorial and midlatitude north Pacific. The model is nonlinear, contains both radiation and a moisture budget with associated precipitation and surface evaporation, and utilizes a linear balance dynamical framework. The SSTA experiments are described in detail in Section 3. Supporting observational analysis of atmospheric planetary waves is briefly summarized in Section 2.

More extensive general circulation models have also been used to consider the problem of the atmosphere's response, especially in the horizontal propagation of planetary-scale waves, to SSTA. Two such studies using the GLAS GCM were done by Shukla and Wallace (1983) and more recently by Fennessy, Marx, and Shukla (1985). One of the primary differences between our two-level model and the multi-level GCM's is the ability to represent vertical propagation of energy and momentum. Should a two-level model with a rigid lid be able to simulate the Walker circulation? This question is addressed in Section 4 of this report.

In December 1982, the Principal Investigator visited Dr. B.N. Goswami at NASA/Goddard Laboratory for Atmospheric Science and learned of the work being done with a symmetric version of the GLAS General Circulation Model. This work was subsequently published in Goswami et al. (1984) and in Goswami and Shukla (1984). The latter paper considered quasi-periodic oscillations in the symmetric GCM.

A few months earlier, John Anderson had joined the project after having completed an M.S. thesis at MIT consisting of an observational study of the zonally symmetric component of the 40-to 50-day oscillation. Given the intent of this research - namely, to foster interaction among diagnostic observational studies, comprehensive GCM's, and simple modeling of planetary-scale phenomena - we embarked on an investigation of a possible dynamical mechanism for the 40-to 50-day oscillation. This mechanism involves the excitation of linear normal modes of a basic state which includes a Hadley circulation as well as a mean zonal flow. Section 5 summarizes our study of slow oscillations in the tropical atmosphere.

Section 6 contains the references for this report.

Section 7 lists the publications that have resulted from this NASA grant. Section 8 consists of a full set of these publications as attachments to this final report.

## 2. Diagnostic Study of Planetary Waves

In this section we focus on the variability in the forcing of ultralong and long planetary waves in the Northern Hemisphere, as determined from observations.

In a paper by Reiter and Westhoff (1981), recent climate trends derived from 28 years of upper air data were described. These data revealed a rather significant trend in the planetary-wave patterns of middle latitudes in the Northern Hemisphere, especially during winter (Fig. 2-1). That trend pattern indicates a deepening of the trough over the central North Pacific, an intensification of the high-pressure ridge over the U.S. west coast, and again a deepening of the trough over eastern North America. As a consequence of the latter feature the eastern United States has experienced a sequence of abnormally cold winters during the recent past.

An analysis of 500-mb pattern differences between months with abundant precipitation in the equatorial Pacific, and months with dry conditions in the same region shows a similarly enhanced precipitation pattern (Fig. 2-2). Most of these strong precipitation episodes tend to occur during the Northern Hemisphere winter and are associated with El Niño (Reiter, 1981, paper presented at the Symposium on Variations in the Global Water Budget, Oxford, England).

The similarity between Figs. 2-1 and 2-2 provides an explanation for the long-term trends in the frequency of equatorial Pacific precipitation surges (Fig. 2-3) and of El Niños, and also in the quasi-periodicity of the southern oscillation (SO): Since 1963 and before the early 1930's, precipitation surges and the SO seem to have occurred with almost biennial regularity. During the time span in between only two
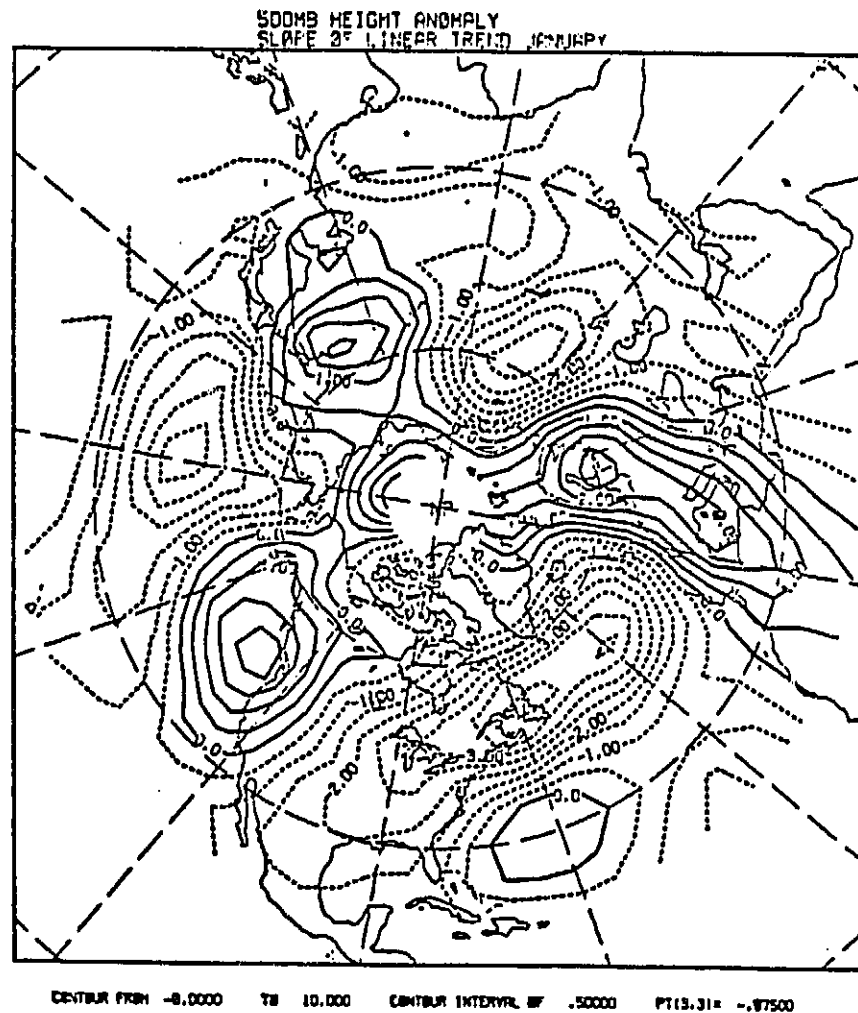
Fig. 2-1   Slope (in gpm/year) of the linear trend 1951-1978 of the 500-mb surface in January. Trend of decreasing heights: dashed; trend of increasing height: solid lines. Trends are different from zero slope by more than two standard deviations in the centers of the fall and rise areas over the central North Pacific, northern Canada, and the eastern USA, and northern Siberia.

FUNCTION= 1 LEVEL= 500 YEAR= 51
TIME= -1/ 0

CONTOUR FROM -180.00 TO 180.00 CONTOUR INTERVAL OF 10.000 PT(3,3)= 20.105
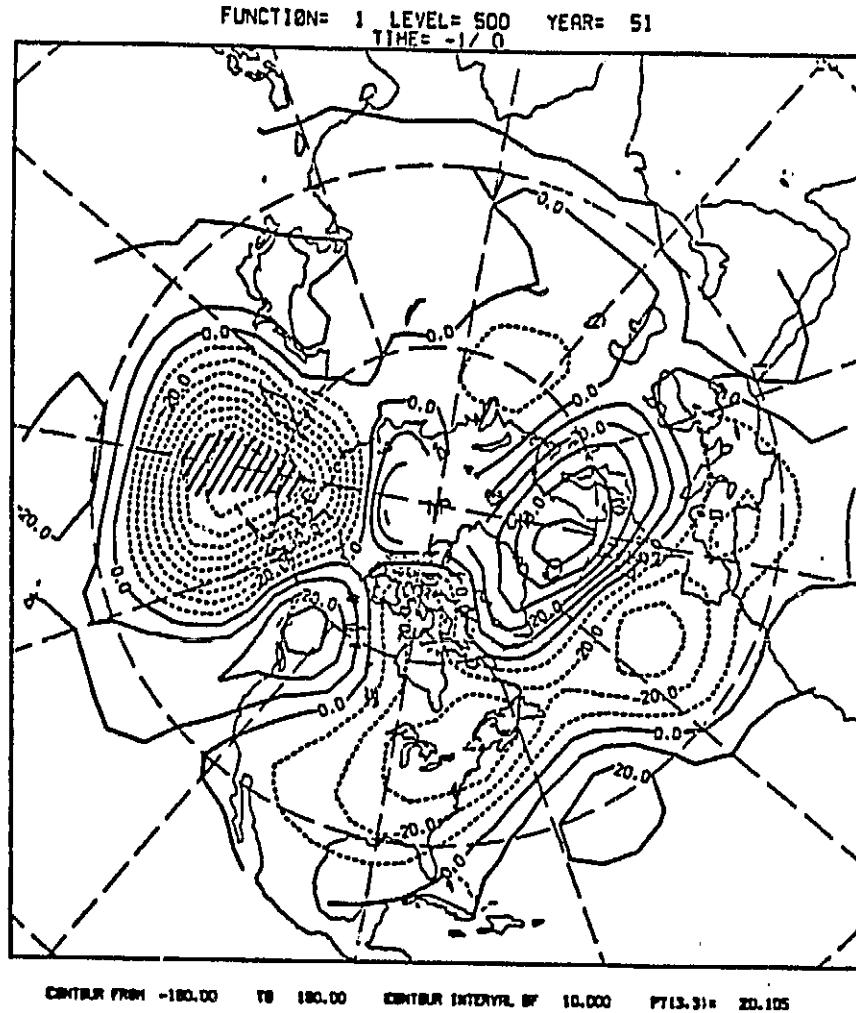
Fig. 2-2   Mean 500-mb height anomalies averaged with respect to key months 8/51, 11/53, 4/56, 12/57, 4/59, 2/61, 2/64, 9/65, 11/68, 11/72 (precipitation maxima at Line Islands) minus average with respect to key months 10/52, 5/54, 2/56, 2/57, 11/58, 2/61, 6/64, 4/67, 5/68, 7/70, 7/73, 8/75 (precipitation minima at Line Islands). 500-mb difference patterns are shown with -1 month lag against the aforementioned key months. Analysis interval: 10 gpm. The hatched region indicates confidence > 99% that two different ensembles were differenced.

Fig. 2-3  Time series of Line Islands precipitation index.  Small dots indicate monthly values, line stands for seven months running-mean smoothing.

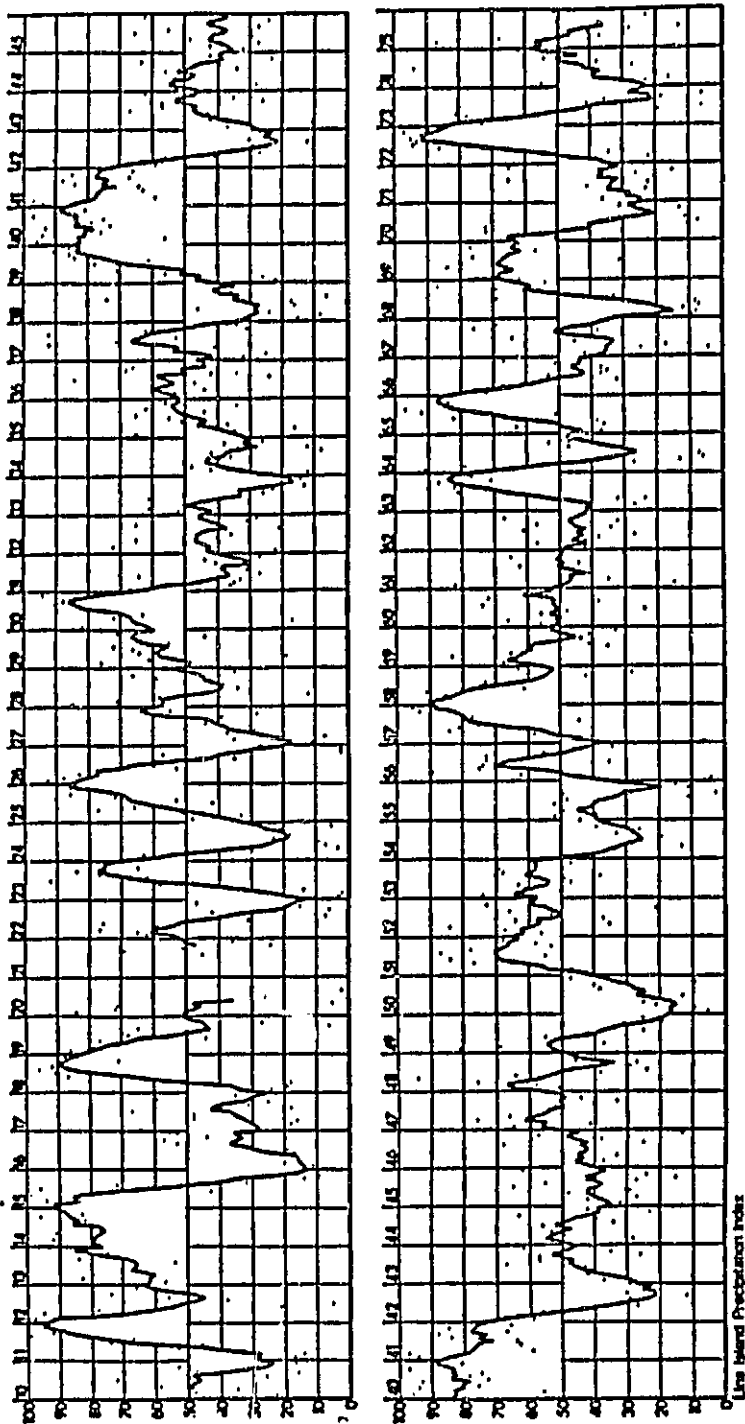major surges were observed - one in 1940-42 and one in 1957/58. The increased frequency in precipitation surges during recent years goes well with the enhanced planetary-wave pattern and the cooling trend over the central North Pacific (Fig. 2-1).

A linear numerical model described by Hoskins and Karoly (1981) shows that tropical heat sources (such as the release of latent heat in equatorial Pacific precipitation surges) would result in patterns of standing Rossby waves similar to the ones shown in Figs. 2-1 and 2-2.

We, thus, have established at least one scenario in which a specific heat source and sink distribution results in a large-amplitude quasi-stationary wave pattern which has a considerable impact on local climates mainly over the United States and Europe. This distribution is characterized by a latent heat source in the equatorial Pacific and by a heat sink in the central North Pacific [where deep troughs are tied in a feedback process to cold sea surface temperature (SST) anomalies]. The amplified ridge over the Rocky Mountains would suggest that such a wintertime heat source and sink distribution lies in a near-resonance configuration with orographically forced planetary waves.

3. Short-Term Climate Fluctuations Forced by Thermal Anomalies in a Two-Level Model

3.1 Introduction

Numerical models are an important tool for testing certain hypotheses concerning climate variability. During recent years a wide variety of models have been developed. Complexity of such models ranges from the simple energy balance models (e.g. Budyko, 1969; Sellers, 1973) to the multi-level primitive equation models (e.g. Manabe et al., 1965; Kasahara and Washington, 1971; Corby et al., 1977; Otto-Bliesner et al., 1982).

Intermediate complexity models (Kikuchi, 1969; Salmon and Hendershott, 1976; Held and Suarez, 1978), with reasonable dynamical and physical simplifications, can simulate some aspects of the largest scales of atmospheric motion. The computational economy of such models provides the opportunity for longer periods of simulation and for more extensive testing of physical and dynamical processes. Moreover, such models can provide a first insight into atmospheric problems before using the complicated general circulation models. Also, intermediate complexity models are useful for interpreting the results of more complicated models (Chervin et al., 1980).

Observational studies, such as those by Bjerknes (1969) and Namias (1976), suggested that sea surface temperature anomalies (SSTAs) in the equatorial and midlatitude Pacific, separately, could influence the atmosphere during the subsequent month or season. Horel and Wallace (1981) defined the midtropospheric geopotential height pattern associated with seven warm-water episodes between 1950 and 1980 in the equatorial central and eastern Pacific.

The southern oscillation (SO) is defined as the tendency of sea level pressure anomalies in the South Pacific Ocean to be of opposite sign from those in the Indian Ocean and Indonesian region (Walker and Bliss, 1932; Berlage, 1966; Troup, 1965). Apparently the SO, which has a period around 4 to 6 years, derives its memory from the positive SSTAs in the equatorial East Pacific. On occasion, these warm-water episodes are linked to the El Niño phenomenon off the coast of Peru. This phase of the SO is defined as a low or negative index. In such situations, the South Pacific Convergence Zone is pushed from its mean position towards the equator, and the Intertropical Convergence Zone moves into a near equatorial position (Ramage, 1975; Trenberth, 1976). The equatorial dry zone east of $160°E$ experiences one of its prolonged precipitation surges (Reiter, 1978, 1979).

Climate sensitivity experiments have been performed using a variety of numerical models to investigate and test the different arguments proposed by observational studies. The complexity of such models ranges from linear models (e.g. Egger, 1977; Hoskins and Karoly, 1981) to multilevel nonlinear general circulation models (e.g. Rowntree, 1976; Chervin et al., 1976; Keshavamurty, 1982). Most of the numerical results confirmed the response of the atmosphere to equatorial SSTAs. In contrast, middle latitude SSTAs gave relatively weak signals (Chervin et al., 1980). However, these results do not negate possible effects of midlatitude SSTAs. Hendon and Hartmann (1982), using a global, steady state linear model, concluded that midlatitude SSTAs might be of equal or greater importance than tropical forcing in altering planetary wave patterns. In their model the remote response was severely damped as a result of either Rayleigh friction, Ekman pumping or the inclusion of sensible heat feedback.

In the present study we developed a two-level, global, spectral model (Hanna, 1982) to test the effects of north-south SSTA gradients between the equatorial and midlatitude North Pacific. The model is a nonlinear, quasi-geostrophic (linear balance) model. The advisability of a global rather than a hemispheric geometry arises from the fact that the latter can produce anomalous Rossby waves which could crucially affect our study (Roads and Somerville, 1982). Also, nonlinear interactions could be of some significance. In a linear model the mean zonal flow is specified and the linear solutions are nearly resonant (Frederiksen and Sawford, 1981). A nonlinear model allows the mean flow to interact with the perturbations, and the solutions are not near the resonant state.

## 3.2 Basic structure and physical forcing of the model

The two levels representing the model's atmosphere are 750 mb and 250 mb. The surface is assumed at 1000 mb. The model retains the nonlinear interactions between dependent variables. Such interactions are important components of midlatitude synoptic motions. The present model uses a moisture budget equation at the 750 mb level with moist convective adjustment between the two layers. The advection by the divergent wind is retained, and static stability is allowed to vary with time and geographical location.

The physical forcing is parameterized with reasonable simplicity to include the major forcing mechanisms which develop the large scale atmospheric circulation. The solar energy is specified as a function of latitude and time assuming a daily mean zenith angle (Wetherald and Manabe, 1972). The amount of solar energy absorbed by the model's atmosphere and the earth's surface is calculated using a formula given by

Kubota (1972). Calculation of the long-wave radiative cooling of the model's atmosphere makes use of a parameterization of the outgoing infrared radiation (Thompson and Warren, 1982), whereas the net long-wave irradiance at the surface is calculated following Deardorff (1978). The mechanical effects of orography are introduced in the form of a lower boundary vertical velocity. The differential diabatic heating due to the distribution of land and sea also is included. The sea surface temperatures are specified using the observed January mean values. On continents and ice surfaces the thermal energy balance equation is solved for the surface temperature. Both orography and differential heating between land and sea are important for producing correct phases and amplitudes of the middle latitudes ultralong waves (wave numbers 1 to 4) in linear atmospheric models (Sankar-Rao and Saltzman, 1969; Bates, 1977).

The upper layer is heated by short and long-wave radiation, by lateral diffusion of heat, and by the heat released by convective adjustment. The lower layer is heated by short and long-wave radiation, lateral diffusion of heat, sensible heat flux from the surface, and latent heat release due to condensation, and is cooled by the heat transferred upward by the convective adjustment. Evaporation from the surface is the only source of moisture to the lower layer. Condensed water is assumed to fall as precipitation, without any reevaportion into the lower layer.

A relevant extension, not yet attempted, is the parameterization of upper level clouds and their associated radiative effects. Such future work is envisaged for studying the role of high clouds in short-term climate changes and in the earth's radiation budget.

In the horizontal domain the dependent variables are expanded in terms of spherical harmonics. A rhomboidal spectral truncation is assumed (truncated at zonal wave number 9).

## 3.3 Model equations

The dependent variables representing the linear balance system of equations are: $\psi+\tau$, the stream function at 250 mb; $\psi-\tau$, the stream function at 750 mb; $\theta+\sigma$, the potential temperature at 250 mb; $\theta-\sigma$, the potential temperature at 750 mb; $\chi$, the velocity potential at 750 mb and q, the mixing ratio at 750 mb. The two-level linear balance system of equations with topographic forcing and a moisture budget is given by

$$\frac{\partial}{\partial t}(\nabla^2\psi) = -J(\psi,\nabla^2\psi+f)-J(\tau,\nabla^2\tau)-\tfrac{1}{2}\nabla\cdot(f\nabla\chi_s)-\frac{k_s}{2}\nabla^2\psi_s+k_h(\nabla^4\psi+2\frac{\nabla^2\psi}{a^2}), \quad (1)$$

$$\frac{\partial}{\partial t}(\nabla^2\tau) = -J(\psi,\nabla^2\tau)-J(\tau,\nabla^2\psi+f)+(\nabla\cdot f\nabla\chi)-\tfrac{1}{2}\nabla\cdot(f\nabla\chi_s)+\frac{k_s}{2}\nabla^2\psi_s$$

$$-2k_d\nabla^2\tau+k_h(\nabla^4\tau+\frac{2}{a^2}\nabla^2\tau), \quad (2)$$

$$\frac{\partial\theta}{\partial t} = -J(\psi,\theta)-J(\tau,\sigma)+\nabla\cdot(\sigma\nabla\chi)-\tfrac{1}{2}(\nabla\chi_s\cdot\nabla\theta+\nabla\chi_s\cdot\nabla\sigma+3\sigma\nabla^2\chi_s)+k_h\nabla^2\theta+\bar{Q}, \quad (3)$$

$$\frac{\partial\sigma}{\partial t} = -J(\psi,\sigma)-J(\tau,\theta)+\nabla\chi\cdot\nabla\theta-\tfrac{1}{2}(\nabla\chi_s\cdot\nabla\theta+\nabla\chi_s\cdot\nabla\sigma-\sigma\nabla^2\chi_s)+k_h\nabla^2\sigma+\hat{Q} \quad (4)$$

$$\frac{\partial q}{\partial t} = -\nabla\cdot(\underline{v}_1 q)+E-P_c+k_h\nabla^2 q, \quad (5)$$

$$bc_p\nabla^2\theta = \nabla\cdot(f\nabla\tau), \quad (6)$$

$$\Lambda P\nabla^2\chi_s = -J(\psi-\tau,P_g), \quad (7)$$

$$\psi_s = \psi-1.6\tau, \quad (8)$$

where $b = \frac{1}{2}[(3/4)^K - (1/4)^K]$,

$$\bar{Q} = \frac{1}{2} [(4/1)^K Q_3 + (4/3)^K Q_1]/c_p,$$

$$\hat{Q} = \frac{1}{2} [(4/1)^K Q_3 - (4/3)^K Q_1]/c_p,$$

a is the radius of the earth, $c_p$ is the specific heat at constant pressure, R is the gas constant, $\kappa = R/c_p$, f is the Coriolis parameter, $\psi_s$ is the surface stream function calculated by linear extrapolation with respect to height (Salmon and Hendershott, 1976), $\underline{v}_1$ is the horizontal velocity vector in the lower layer, $\chi_s$ is the surface velocity potential which represents the effect of topography, $P_o$ is the lower boundary pressure level ($\equiv$ 1000 mb), $\Delta P = \frac{1}{2}P_o$, $P_g$ is the pressure at terrain height, $P_c$ is the precipitation rate, E is the evaporation rate, $Q_3/c_p$ and $Q_1/c_p$ are the diabatic heating rates per unit mass of the upper and lower layers, respectively.

The frictional dissipation terms are calculated following Lorenz (1961), assuming

a) surface frictional drag is proportional to the flow in the surface layer,

b) friction between the two layers is proportional to the difference between the flow of the two layers.

The lateral eddy diffusion coefficient is given by; $k_h = 1 \times 10^5$ m$^2$ sec$^{-1}$ (Phillips, 1956). The friction coefficients are given by $k_s = 4 \times 10^{-6}$ sec$^{-1}$ (Kikuchi, 1969), and $k_d = 5 \times 10^{-7}$ sec$^{-1}$ (Charney, 1959).

When computing $P_g$, the continental elevations smoothed over 5° latitude by 5° longitude are used (Berkofsky and Bertoni, 1955) assuming a standard atmosphere.

## 3.4  Experimental design

The numerical experiments were designed to investigate possible teleconnections between SSTAs and the atmospheric circulation in the subsequent month or season. During the normal January and February integrations (control runs) the sea surface temperatures were fixed, allowing no time change. The values specified were the climatological means of January. We assumed a negligible change of sea surface temperatures between the two months.

Anomaly experiments started from the initial state on the first of January (day 121). The experiments were continued through the rest of January and February.

### a.  Statistical significance of the signal

The purpose of any statistical significance testing is to provide an estimate of the probability that a given experimental result can be attributed to a specific forcing or perturbation applied in the experiment. In general, any perturbations in the initial conditions or in the forcing of the model will cause a change in the values of the predicted variables. It is then essential to estimate the inherent variability of the model itself. This estimate entails an assessment of the random variations caused by the model's internal, nonlinear dynamics (noise). If the variability of the model's atmosphere due to the effect of SSTAs is not contained within this noise level, then it is considered to be the manifestation of a significant signal.

For estimating the noise level of the model a set of runs was performed to simulate the same period of integration covered by the control case. Each run was done by starting from a different initial state. The initial state at the beginning of January was altered by

assuming the predicted values at the end of the month as initial conditions. This process was repeated successively four times. Variances of temperature and geopotential height were caluclated from four independent runs together with the control run to give four degrees of freedom.

We define the time average of the variable $X_{ij}$ at a grid point i,j to be $\bar{X}_{ij}$, and the ensemble average over five runs of this time average to be $\bar{\bar{X}}_{ij}$. The geographic variance for the variable X can be calculated from the relation

$$(St)^-_{ij} = \frac{1}{4} \sum_{K=1}^{5} ((\bar{X}_{ij})_K - \bar{\bar{X}}_{ij})^2. \tag{9}$$

The standard deviation, $(St)_{ij}$, at each grid point is the positive square root of expression (9).

The difference between the monthly average anomaly experiment and the control run value at each grid point gives the response of the atmosphere to the specified anomaly. This difference is given by

$$\Delta X_{ij} = ((X_{ij})_2 - (X_{ij})_1), \tag{10}$$

where the subscripts 2 and 1 define the anomaly and control cases, respectively.

The significance of the response is calculated using the relation,

$$\xi_{ij} = \frac{\Delta X_{ij}}{(St)_{ij}} \tag{11}$$

The significance ratio ($\xi_{ij}$) should be larger than unity for a signal to be significant; i.e., the absolute value of the difference caused by the anomalies must be larger than the inherent variability of the model. The larger the value of $\xi_{ij}$, the more confidence we have that the observed change is a result of the effect of the anomalous forcing.

According to Chervin and Schneider (1976), $\xi_{ij} \geq 4$ is sufficient for a 5 percent significance level, which means that the probability of such a response arising from mere chance sampling is less than 5 percent.

b. Position and magnitude of the anomalies

The first experiment (Experiment 1) was designed to investigate the effect of warm SSTAs in the tropical Pacific. These warm-water episodes, which last for an average of 16 months near the coast of Peru, have been found to have significant teleconnections with middle latitude weather (Bjerknes, 1969; Rowntree, 1972). This experiment enables us to identify the response of the present model (linear balance) to perturbations in the tropical atmosphere. The SSTA used here has a maximum of 4°C (Fig. 3-1a), closely resembling the observed SSTA in this region.

Experiment 2 respresented a coupled SSTA pattern in the north and equatorial Pacific (Fig. 3-1b). The cold SSTAs in the North Pacific were exaggerated to a certain extent by considering the values in degrees Celsius rather than degrees Fahrenheit (maximum negative anomaly 4°C). In addition, a small area of warm anomaly was located west of the United States. This anomaly distribution closely matches the first eigenvector pattern of monthly mean SSTAs given by Weare et al. (1976). This pattern explains 23 percent of the total sea surface temperature variance.

3.5 Analysis of the results

We decided to show the differences corresponding to February (day 151 to 180). This choice will give the model atmosphere sufficient time to sense and distribute the forcing by the SSTAs. The difference (anomaly minus control) values of the 30-day averages of the temperature and geopotential height fields at the 750 mb and 250 mb levels are analyzed.
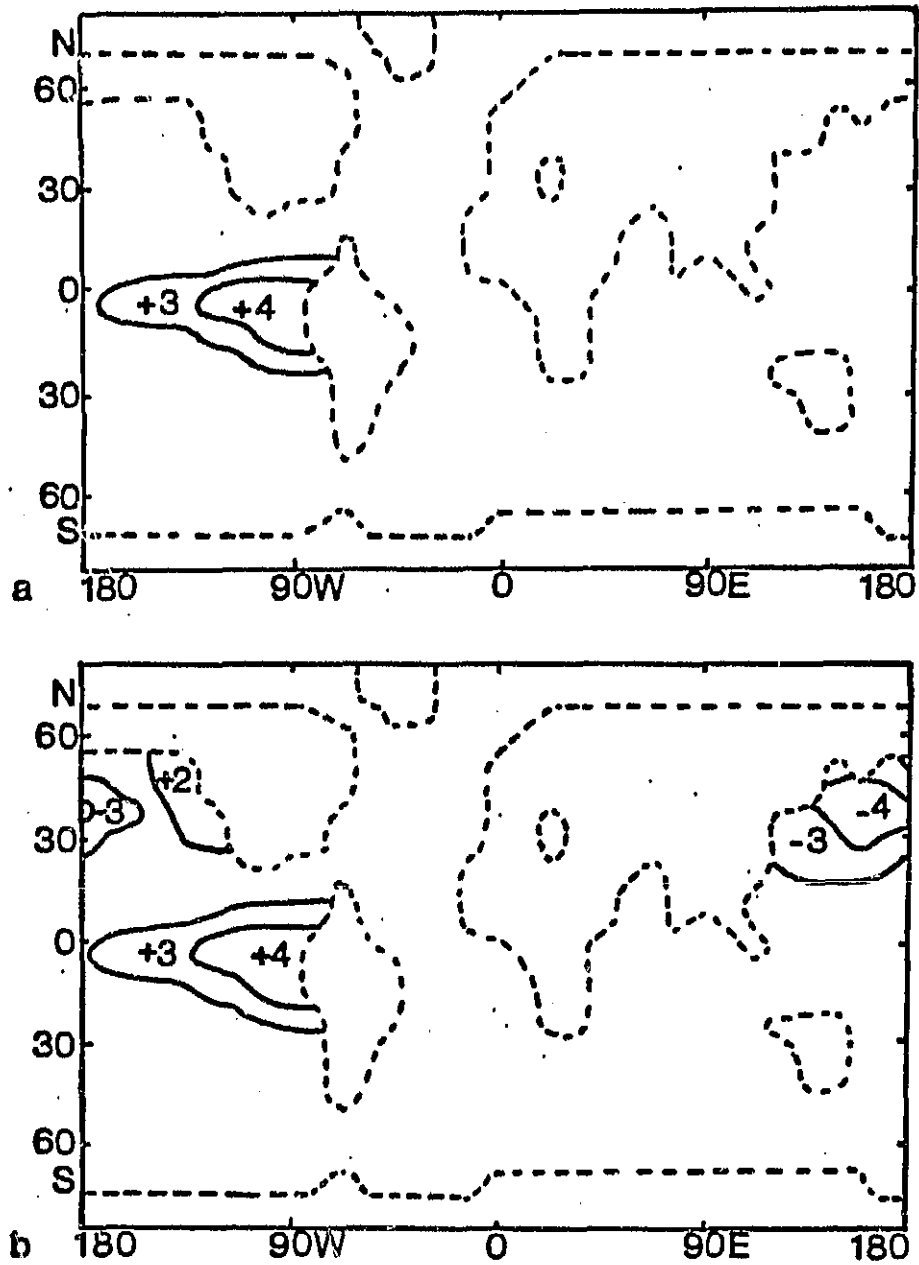
Fig. 3-1    Assumed sea surface temperature anomaly
            distribution (°C) for (a) experiment 1 and
            (b) experiment 2.

The significance of such differences are investigated using the geo-graphic distributions of the standard deviations of the temperature and geopotential height fields. The differences in the zonal averages of the mean meridional transports and variances also are discussed.

a. Warm anomalies in the equatorial Pacific

As mentioned before, in this experiment the positive SSTAs were located in the tropical East Pacific of both hemispheres. It is impor-tant that we analyze the results of this experiment and compare it with the conclusions of primitive equation general circulation models which examined the SSTAs in a similar location. The importance of such analy-ses stems from the use of a linear balance model in our study, which has its limitations in representing the tropical atmosphere.

The differences in the temperature fields (Fig. 3-2) reveal an in situ response of the lower layer of the model atmosphere to the warm anomalies. In comparison, the temperature changes in middle and high latitudes are larger. The largest differences appear to be at 750 mb over the continents of the Northern Hemisphere. There are temperature differences of opposite sign over the western and eastern United States. The same is true for the Eurasian continent where the eastern and west-ern regions display cold temperature as opposed to the warm central region. The middle and high latitudes of the Southern Hemisphere show an east-west temperature wave pattern in response to the positive equa-torial surface temperature anomalies. At the 250 mb level the tempera-ture differences in the South Pacific are almost opposite to those in the lower layers. The differences, at this level, generally are smaller than those in the lower layer.
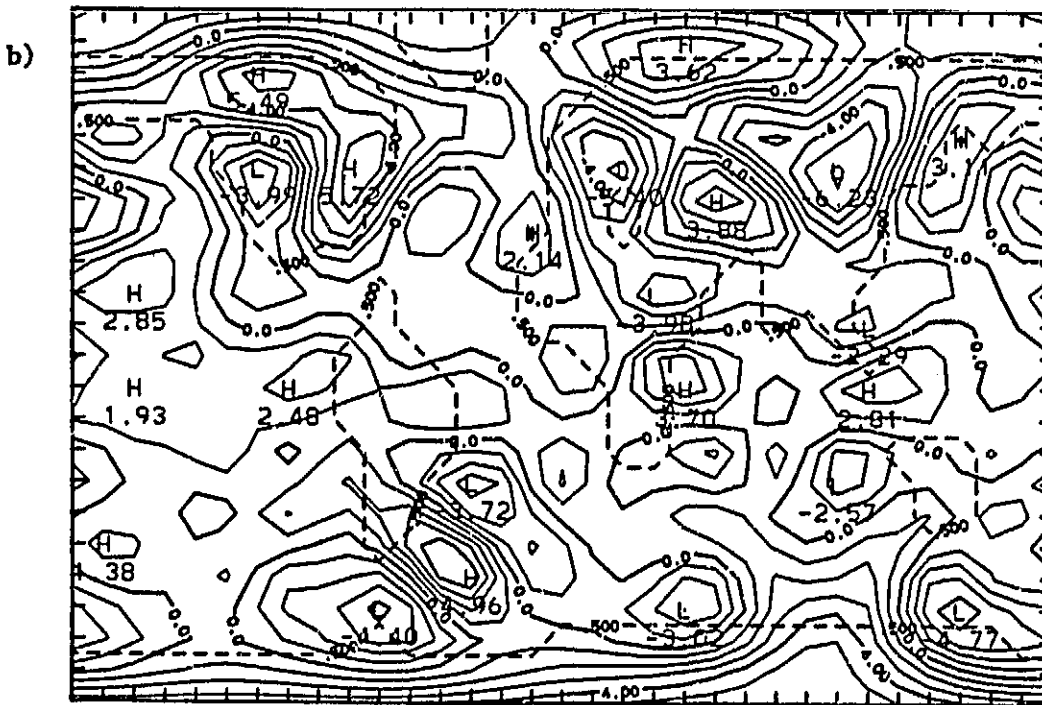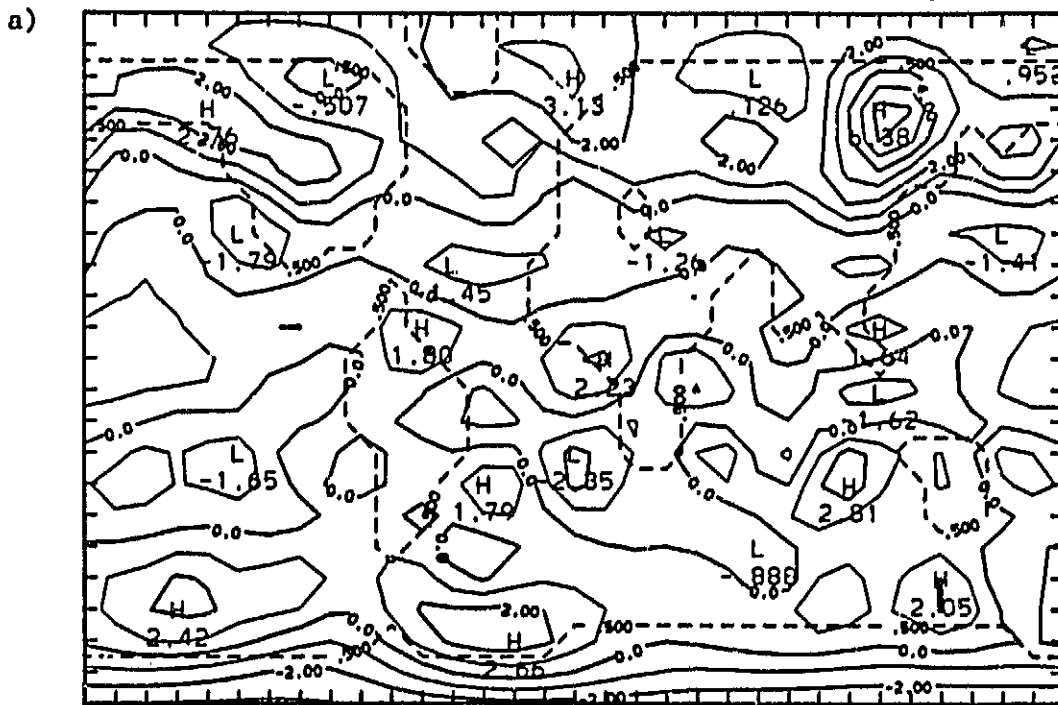
a)



b)



Fig. 3-2    Temperature differences (°C) between the anomaly (experiment 1)
and the control run for February (a) at 250 mb and (b) at
750 mb.

Fig. 3-3b reveals the establishment of a high pressure area over the North American continent at 750 mb. A wave pattern also exists over the Eurasian continent but with smaller differences than over the Pacific Ocean or the North American continent. The negative height differences over the Pacific Ocean agree with the results from a similar numerical experiment done by Rowntree (1976) using the GFDL model. The Aleutian low is deepened and shifted to the east, whereas a low pressure develops near the surface temperature anomaly location. Our own and Rowntree's results support Bjerknes' (1969) hypothesis which states that flow patterns in middle latitude are affected by such tropical SSTAs, trough formation being favored north of the model's tropical sea temperature maximum. The 250 mb geopotential height differences (Fig. 3-3a) show the equivalent-barotropic character of the middle and high latitude atmosphere away from the anomalous forcing area. At the same time, directly above the anomalies we find negative pressure differences in the lower layer and positive height anomalies in the upper layer, hydrostatically consistent with atmospheric warming.

Hoskins and Karoly (1981), using a linear model, concluded that midtropospheric thermal anomalies in the Northern Hemisphere subtropics tend to induce a wave pattern to the northeast. Their results seem to support the observational study by Horel and Wallace (1981). The results of the present experiment, also, seem to support their arguments concerning the establishment of a wave pattern north of the anomalies location. However, a comparison between the geopotential height difference pattern at 250 mb discussed above, and the midtropospheric geopotential difference pattern over North America estimated by Horel and Wallace, indicates a discrepancy in the phases of the observed and
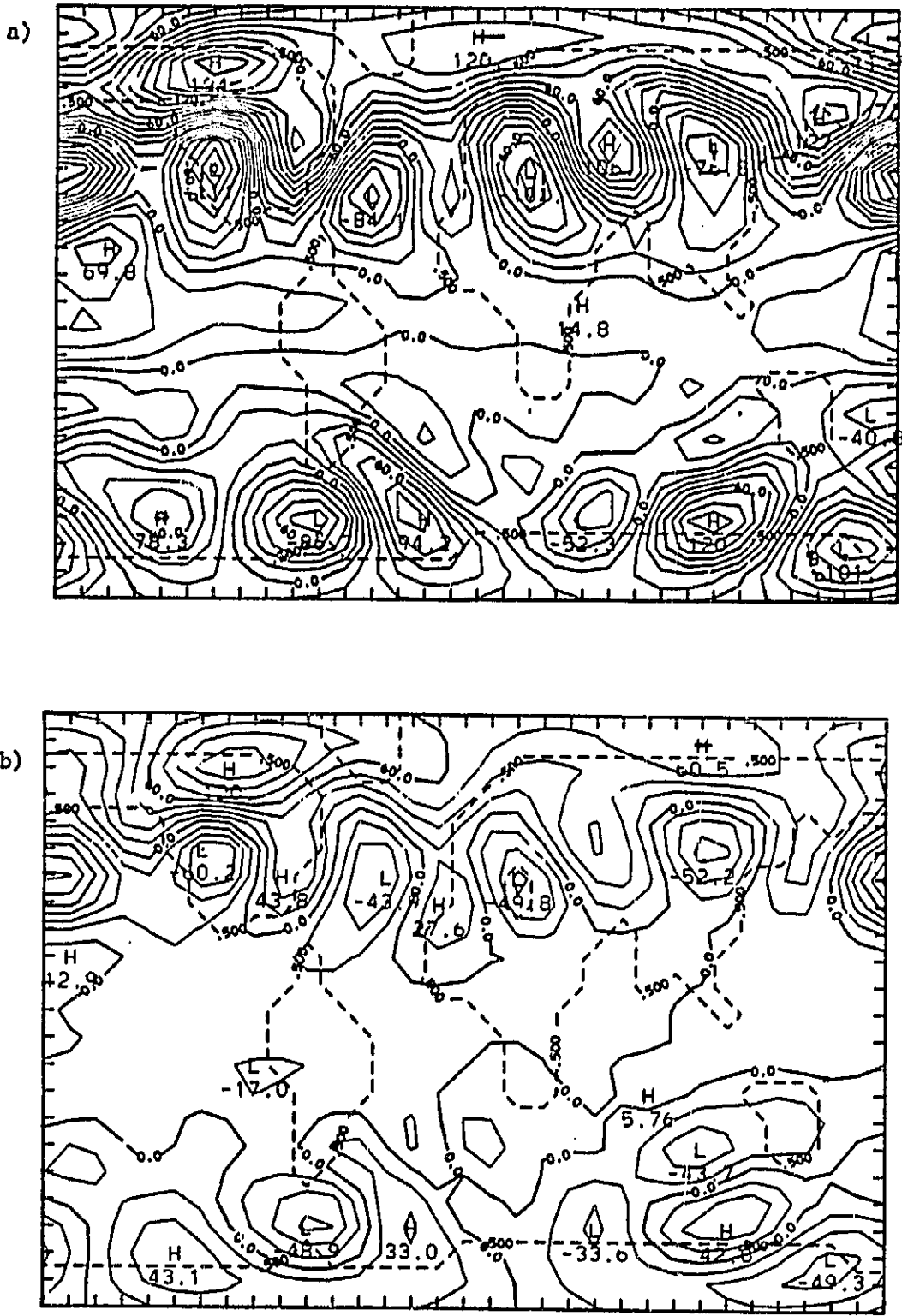
a)



b)



Fig. 3-3   As in Fig. 3-2 but for the geopotential height differences (m).

calculated patterns over the North American continent, especially over the western United States. In particular, we note the penetration of the negative geopotential height anomaly over the western part of the United States.

b.   Coupled cold (north) and warm (equatorial) SSTAs in the Pacific

Experiment 2 was designed to investigate the effects of SSTAs in the north and equatorial Pacific. Since this pattern explains 23 percent of the variances of monthly mean SSTAs, it is important to examine the atmospheric response associated with such a distribution and to see if it supports the anomalous geopotential height pattern proposed by Horel and Wallace (1981).

The differences in the 750 mb temperatures (Fig. 3-4b) show a similar sign of temperature differences near the surface anomalies. The largest differences appear as a pool of cold air over Canada, a warm air mass over Greenland and a cold air mass over northwestern Eurasia. Also, a warm air mass is seen to develop over the southeastern part of the United States. It is of interest to note the relative increase of the temperature differences at this level from the comparable pattern in experiment 1. The Southern Hemisphere high latitudes have smaller differences in the temperature pattern. At 250 mb (Fig. 3-4a), the differences are generally smaller than those in the lower layer, with warm centers above the cold anomalies and vice versa.

The 750 mb geopotential height difference pattern of Fig. 3-5b reveals a ridge over western North America between low pressure centers over the eastern part of that continent and the eastern Pacific. This figure also shows positive geopotential differences over Greenland and a deep trough over Northern Eurasia and its southeastern parts. Again the
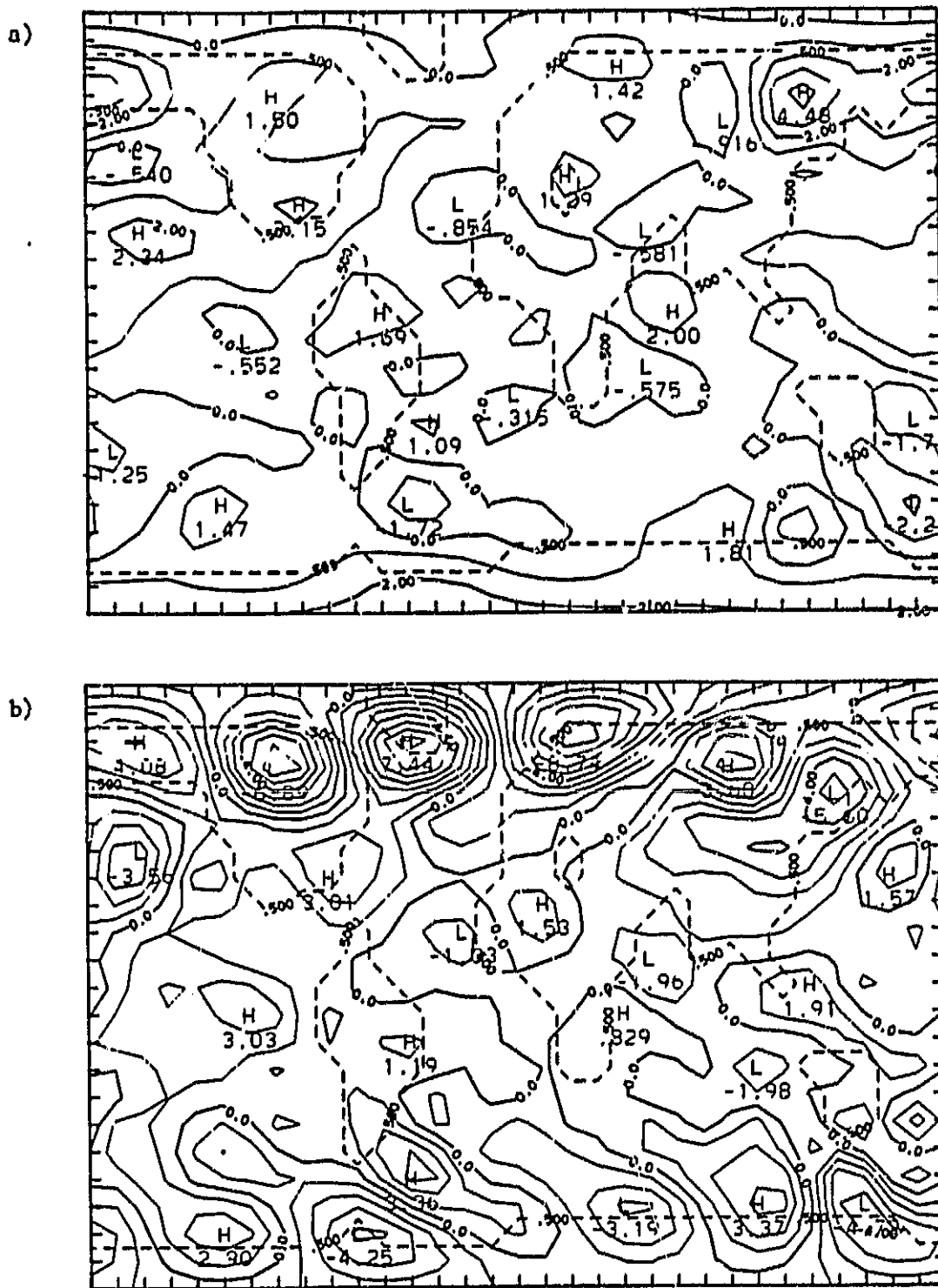
a)



b)



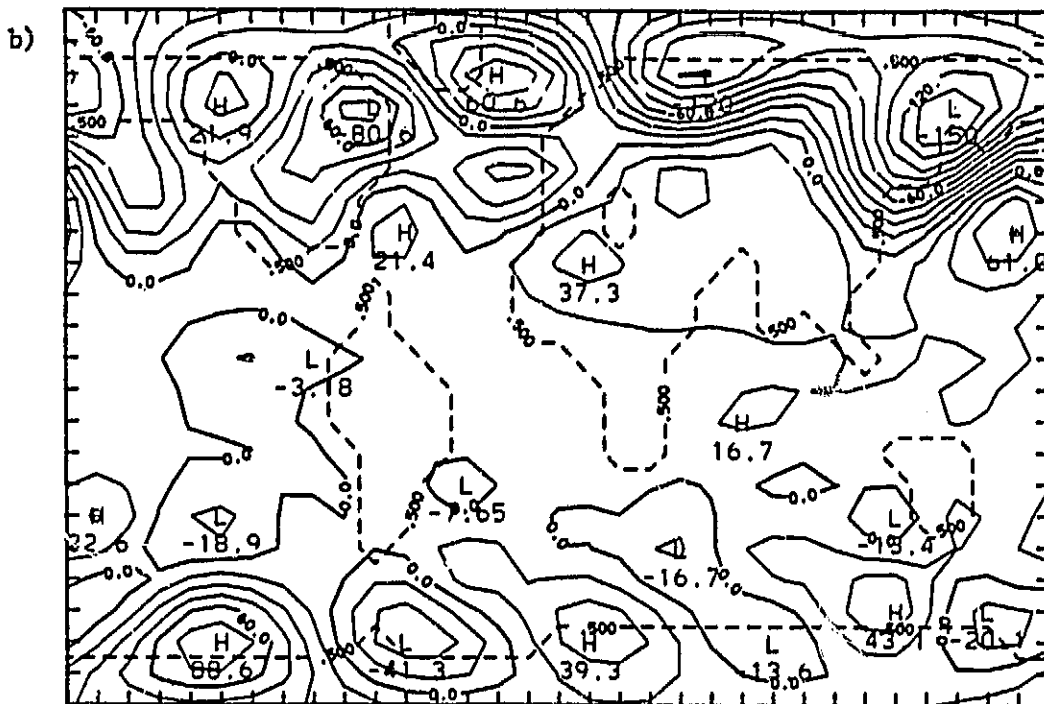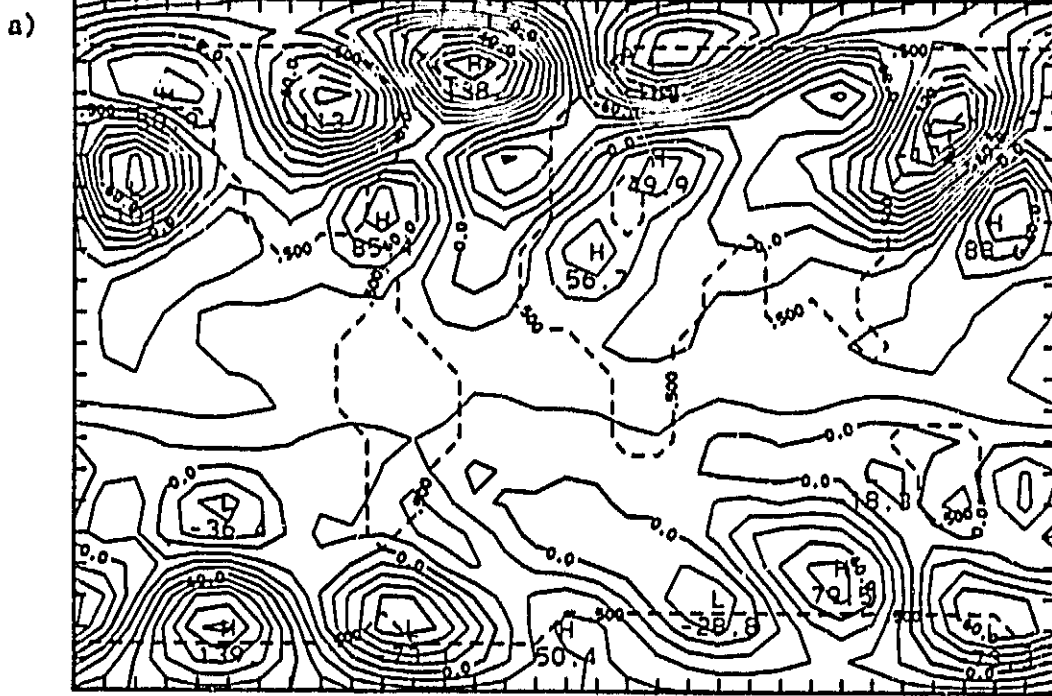Fig. 3-4    As in Fig. 3-2 but for experiment 2.

a)



b)



Fig. 3-5    As in Fig. 3-3 but for experiment 2.

Southern Hemisphere has relatively smaller geopotential height differences than the Northern Hemisphere. The 250 mb geopotential height differences (Fig. 3-5a) show ridging over the western part of North America and Canada together with two negative height anomalies to the east and west and a high pressure anomaly over the tropical Pacific. Not to be ignored is the larger magnitude of negative differences over the northern and southeastern parts of the Eurasian continents. This geopotential height pattern seems to be more relevant to the equivalent pattern given by Horel and Wallace (1981). In other words we believe that the northern Pacific Ocean sea surface temperature anomalies might be essential in producing the correct phase of the observed geopotential height anomaly pattern (Reiter, 1983).

c. Meridional transports initiated by the two anomaly types

To gain more insight into the results of the two experiments, we analyzed the differences (anomaly minus control) in the zonal averages of the northward transports of momentum, sensible and latent heat. Figs. 3-6a, b, c show the differences of transports of momentum, temperature and moisture, respectively, í Experiment 1; their counterparts in Experiment 2 are displayed in Figs. 3-6d, e, f. The differences shown are those resulting from the transient eddies, stationary eddies, the mean meridional circulation and the total of these differences.

The differences in the meridional transport of momentum indicate that the coupled anomaly pattern largely enhances the northward transports resulting from the stationary and transient eddies (Fig. 3-6). The northward transport of momentum dominates the tropical, subtropical and middle latitude belts. In comparison, the El-Niño pattern produces relatively smaller values of the differences, especially for the sta-
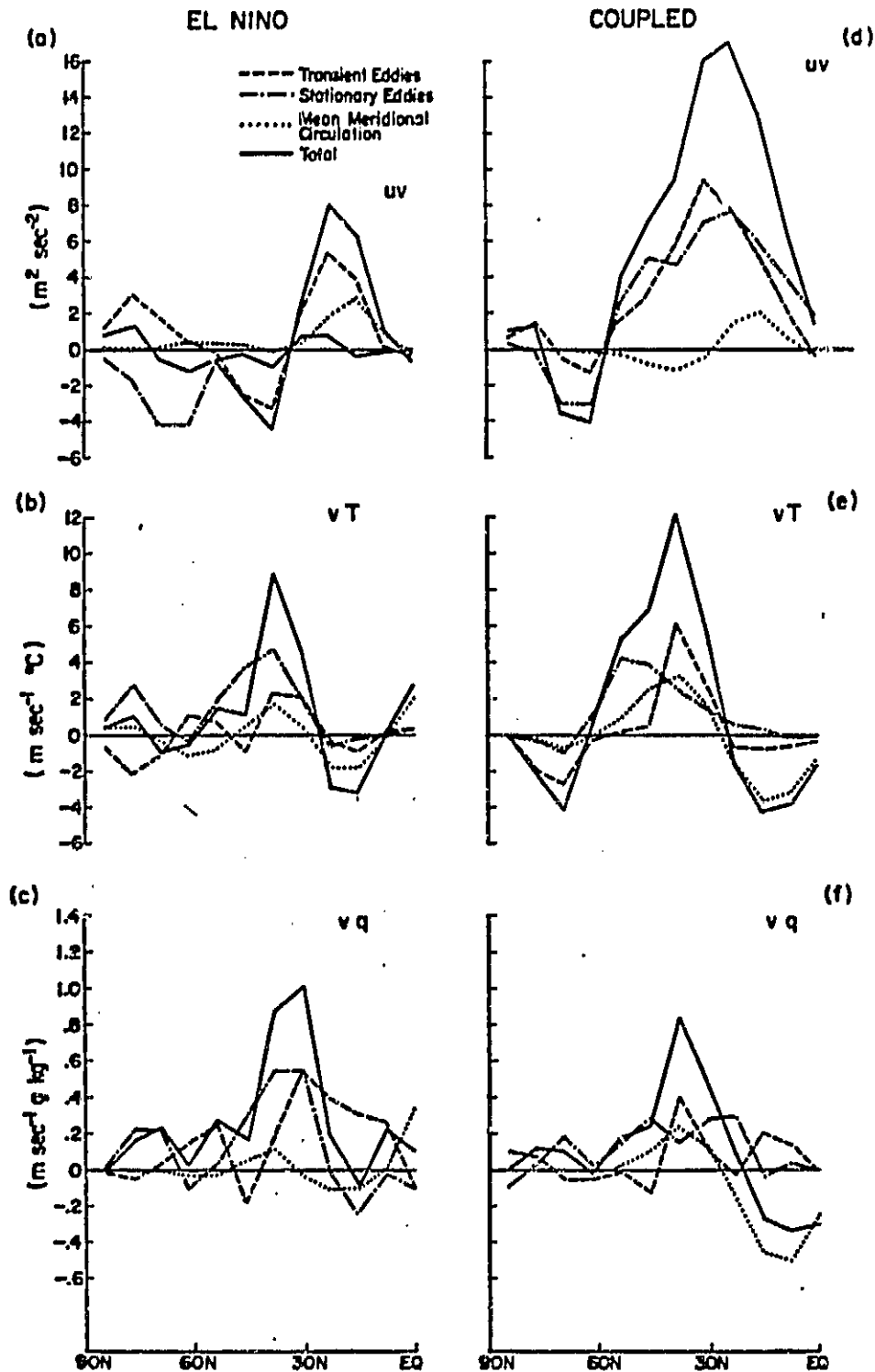
Fig. 3-6  Differences (anomaly minus control) in the zonal average
meridional transports by transient eddies (dashed), by
the stationary eddies (dot-dashed), by the mean meridional
circulation (dotted) and the total transports (solid):
(a) westerly momentum (experiment 1); (b) temperature
(experiment 1); (c) water vapor (experiment 1); (d) westerly
momentum (experiment 2); (e) temperature (experiment 2)
and (f) water vapor (experiment 2).

tionary component. The differences in the northward transport of momentum resulting from the mean meridional circulation are comparable between the two anomaly patterns. The total differences in the meridional transport shows that the value of the maximum transport at 23°N in case of the coupled pattern is nearly double that pertaining to the case of the El-Niño pattern.

The differences in the northward transport of temperature (Figs. 3-6b,e) show that the middle latitude transient eddies are more active with the coupled SSTA patt n. In the case of the coupled pattern, the heat transport by the mean meridional circulation is larger in the tropical and subtropical latitudes. The differences in the transports by the stationary eddies do not indicate much change between the two anomaly patterns except, for the location of the maximum transport. As in the case of the differences in the momentum transport, the total meridional transport of temperature is larger for the coupled anomaly than for the El-Niño pattern.

The differences in the transports of moisture (Figs. 3-6c, f) do not show the same features of the momentum and temperature transports. In general, the differences in the meridional transports by the stationary and transient eddies are larger for the El-Niño pattern than for the coupled pattern, while for the mean meridional circulation the opposite is true. The total differences in the northward transport of moisture do not show a large difference between the two anomaly patterns except in the tropical latitudes where the coupled pattern causes a strong southward transport of moisture.

## 3.6 Determination of the noise level

It is important to determine the noise level of the model-generated climatology statistics in order to judge the significance of the re-

sponses calculated by the two experiments. Analyses of the standard deviations of the temperature and geopotential height fields at 750 mb (Fig. 3-7a, b) reveal that the variability is mostly in middle and high latitudes of the Northern Hemisphere (winter hemisphere). This preponderance of variability is a result of the enhanced transient eddies in that hemisphere. The values decrease equatorward in both hemispheres. The maximum variability of temperature is found between 50°N and 70°N to the west of Canada and to the east of Asia. This feature is in qualitative agreement with observations by Crutcher and Meserve (1970) for the 850 mb temperatures using data from January of 14 years. The relatively small magnitude of variance in our model results can be attributed to the fixed ocean temperature assumption and to the different sample sizes involved. The standard deviations of the geopotential height display similar features as those of the temperature field, but are shifted towards the east. This shift is a result of the baroclinic nature of disturbances propagating through these latitudes.

As we discussed in Section 3.4, a significant atmospheric response with confidence at about 95 percent requires the significance ratio to be $\geq$ 4. A comparison between the standard deviation values and the resulting differences from the previous experiments shows that this condition is fulfilled for most of the maxima and minima revealed in the model-produced patterns. This test guarantees that the differences which result from the thermal anomalies exceed (by at least four times) the differences caused by the random variability of the model itself.

3.7 Summary and conclusions

We have investigated the atmospheric response to equatorial and midlatitude SSTAs. A two-level global spectral model which retains
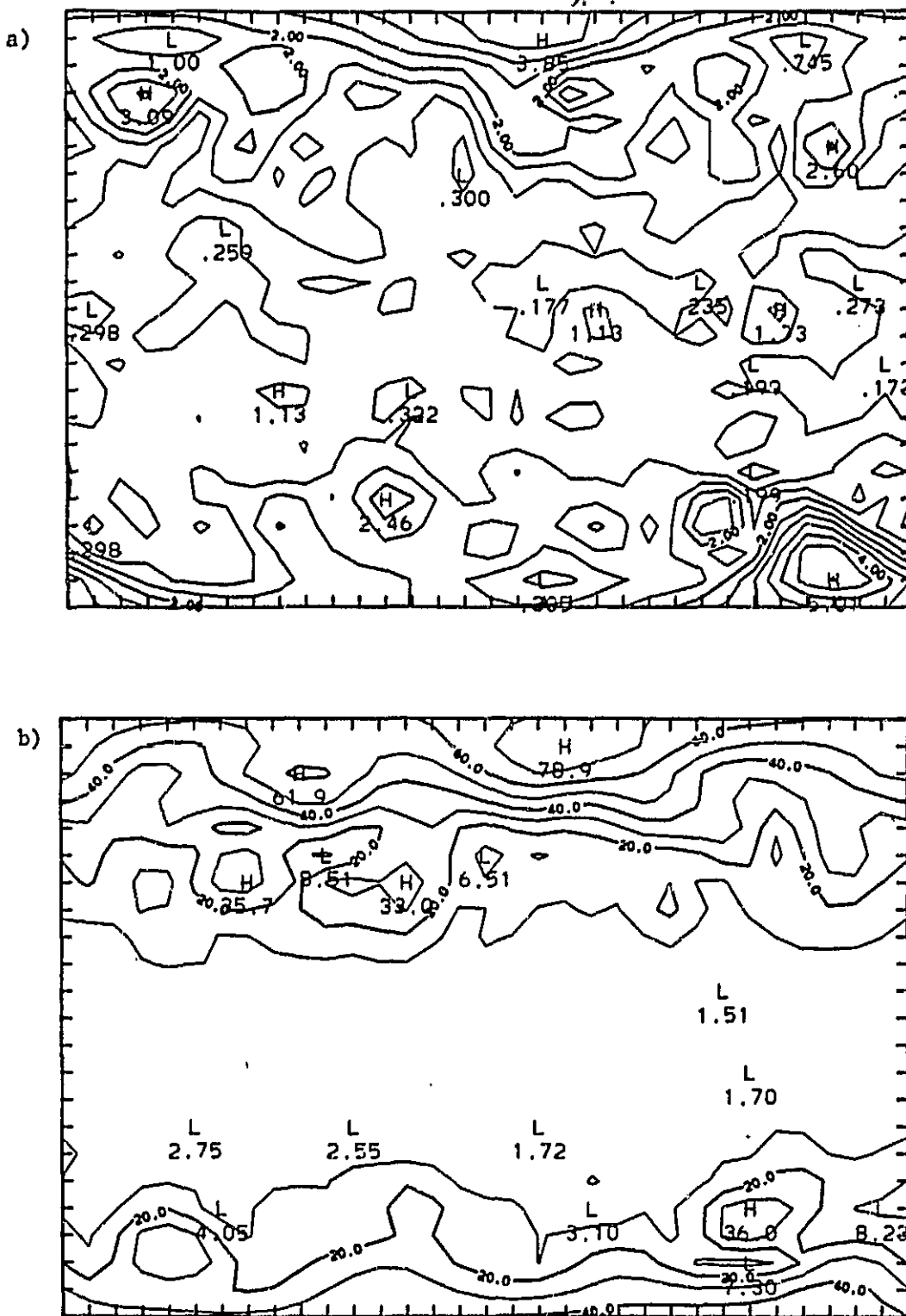
Fig. 3-7    Geographical distribution of the standard deviations (St)$_{ij}$
from five February runs simulated by the model (a) 750mb
temperature (°C) and (b) 750mb geopotential height (m).

nonlinear interactions was used. Topographic forcing and land-sea differential heating were included.

The results of the two experiments indicate that positive SSTAs in the equatorial Pacific (experiment 1) produce local midtropospheric thermal anomalies. The middle latitude geopotential height pattern shows a significant response to this surface temperature anomaly. However, the resulting geopotential height difference pattern, which is significant, has a different phase than the midtropospheric geopotential height distribution which was suggested by Horel and Wallace (1981), who analyzed observations of the atmospheric geopotential heights associated with the El-Niño. Experiment 2, of this paper, describes the effect of coupled SSTAs in the Pacific. This SSTA pattern explains 23 percent of the variances of monthly mean SSTAs. The resulting midtropospheric geopotential height differences are similar to the anomaly pattern proposed by Horel and Wallace.

Differences (anomaly minus control) in the meridional transports of momentum, temperature and moisture have been analyzed for the two experiments. The analysis results are relevant to the transports of sensible and latent heat, respectively. The analysis indicates the importance of the northern Pacific SSTAs when coupled to the El-Niño SSTAs in the equatorial Pacific. The coupled pattern tends to activate the transports of momentum and sensible heat, especially by transient and stationary eddies. The maximum total differences of transport of momentum is nearly double that revealed from the El-Niño experiment. It is also noted that the latitudinal belts covered by the northward transport are broadened in the case of the coupled SSTAs. The meridional transports of latent heat do not show much difference between the

two SSTA distributions except for the large southward transports of moisture by the mean meridional circulation in the tropical latitudes in case of the coupled distribution (experiment 2).

4.   Theoretical Adequacy of a Two-Level Model of the Tropical
     Atmosphere

In the course of the initial stages of our development of a two-level model, we became aware of a recent investigation of Gill (1980) which is relevant to our study. Gill showed that several important details of the heat-induced tropical circulation called the Walker circulation could be explained with a simple, analytic, two-level linear model. There was some question, however, regarding the validity of such a model for tropical circulations, since there exist internal modes in the tropics, with small positive equivalent depths, which can propagate their energy vertically and therefore out of the tropical troposphere. Should a two-level model with a rigid lid be able to simulate the Walker circulation? This question is relevant to our current study because we also are developing a two-level model with a rigid lid, but one in which the circulations can develop nonlinearly.

The results of our study are presented in Geisler and Stevens (1982). Figure 4-1 shows the vertical profile of zonal wind at three equatorial points east of the center of the diabatic forcing. The distance to the east is given on the figure in kilometers. The diabatic heating is assumed steady; a five-day linear dissipation time scale has been used; and a lid has been placed at 50 km, well above the heating layer within the troposphere (below 16 km). The resultant structure in the zonal flow indicates that the two-level model assumption made by Gill should reasonably simulate the continuous behavior of our model solution.

However, this result holds true only if the dissipation time scale is shorter than the time scale associated with the heating. In this
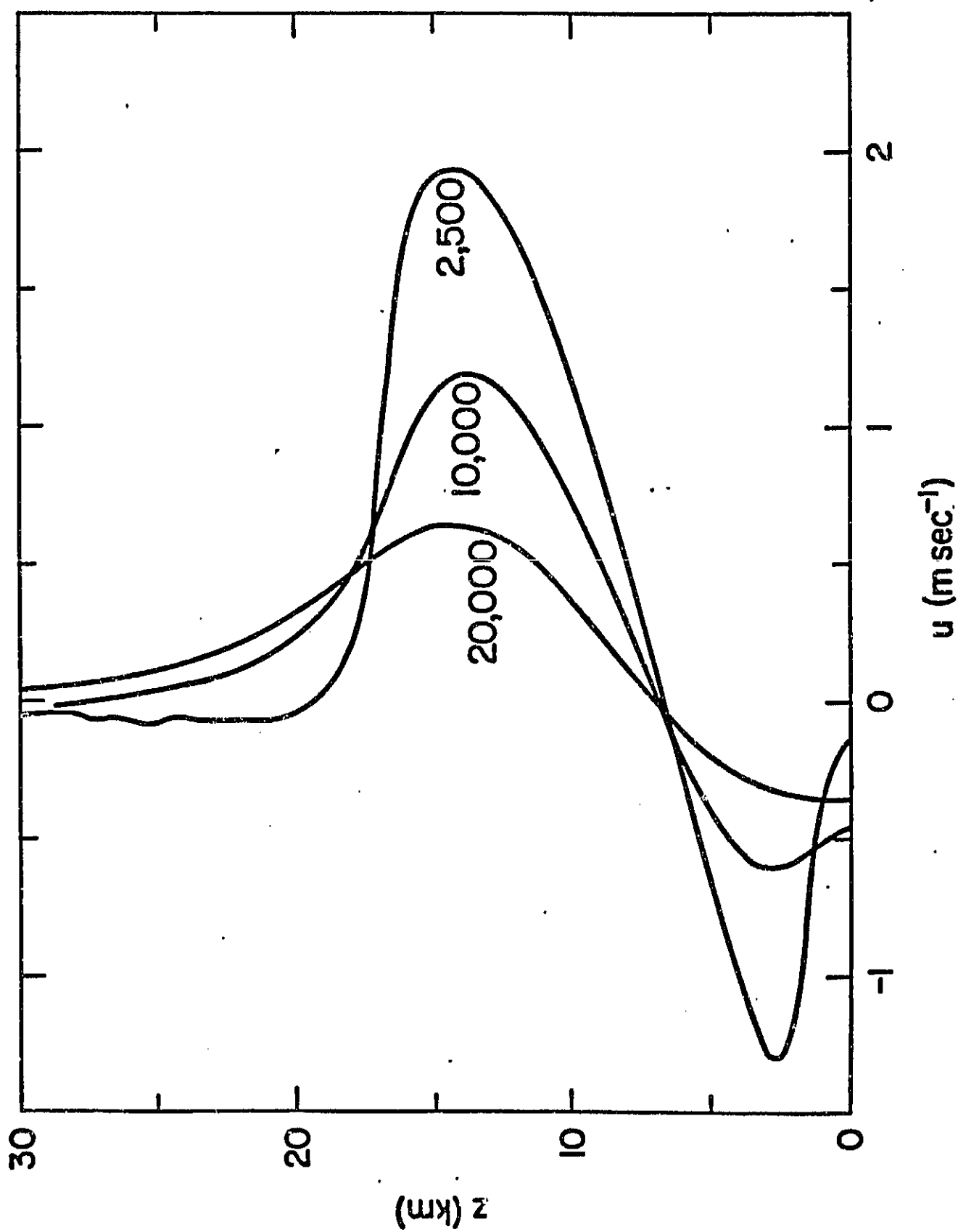
Fig. 4-1   Zonal wind on the equator at three equatorial points east of the center of the forcing.

calculation, the time scale was infinite. As we shortened the time scale of the diabatic forcing and decreased it below the time scale of the dissipation, this result changed drastically. At a frequency of 10 times the dissipation rate, there is large amplitude at upper levels together with a 180-degree phase shift indicative of reflection at the artificial 50-km lid. Hence, a two-level model is not appropriate for tropical circulations that are rapidly changing and nondissipative. This calculation verifies the expectation of linear equatorial wave theory. Stevens, Lindzen and Shapiro (1977) demonstrated that there is a significant amount of dissipation even in the transient tropical disturbances. Therefore, the two-level model may still be appropriate for the "weather" phenomena in the tropics as well as the longer-term "climate". This type of model already has a long and venerable history for midlatitude phenomena.

5.  Forty- to Fifty-Day Oscillation

5.1  Introduction

The presence of quasi-periodic fluctuations in the tropical tropo-
sphere with periods ranging from 40-50 days were first reported by
Madden and Julian (1971).  Since then, observations of these variations
have been reported in a large number of observed tropical meteorological
parameters including winds, surface pressure and observed convective
cloud cover.  Recent diagnostic studies have also reported evidence for
a mid-latitude component of the phenomenon.  The existence of the mid-
latitude component provides new incentive for studying the oscillation
because of its possible role in understanding tropical-midlatitude
interations on these and longer time scales.

In spite of the rather lengthy observational history of the 40-50
day oscillation there have been relatively few dynamical explanations
proposed for the time scale of the motion.  The source of the oscilla-
tion period remains a topic of considerable interest and uncertainty.

In the first report of the oscillation Madden and Julian (1971)
detected the presence of a relatively narrow-band signal with periods of
40-50 days in 850 mb level zonal wind, 150 mb level zonal wind and
surface pressure observations which were taken at Canton Island in the
West Pacific.  The 850 mb winds were observed to be essentially out of
phase with the winds at 150 mb.  An interesting aspect of the Madden and
Julian report is that there was no detectable signal in the 850 mb
mixing ratio field at Canton Island which suggests that the oscillation
was not locally forced by variations in the water vapor content,
although it is possible that the oscillation could be forced further

west in the Indonesian region. This would seem to argue against a mechanism forced from the surface by effects such as variations in sea surface temperature.

Madden and Julian (1972) reported the results of a study designed to determine the spatial structure of the 40-50 day oscillation. In this study they computed the surface pressure cross-spectra of Canton Island with the other available tropical stations. Their results, which are summarized in Fig. 5-1, indicate that the surface pressure effects of the phenomena involve most of the tropics with the possible exception of the Atlantic region. The surface pressure phase analysis shows a strong tendency for the disturbance to propagate away from the equator towards both poles and eastward phase propagation in the Indonesia-Borneo "maritime continent" region. The longitudinal variation of the oscillation is consistent with that of a motion having both zonally symmetric (wavenumber 0) and zonal wavenumber 1 components. Based on the evidence of the observed winds and 700 mb mixing ratio values Madden and Julian proposed an observational description of the phenomenon which consisted of a modulated, eastward traveling convective disturbance in the Indonesia/western Pacific areas. Although they did not detect any extratropical evidence for the oscillation they noted that since the average tropical surface pressure varied with the oscillation phase that the net change in the mass of the tropical atmosphere must be reflected in other regions.

A study similar to the work by Madden and Julian was performed by Parker (1973). Parker, who was apparently unaware of the Madden and Julian work, studied the 100 mb winds in an equatorial band from 10°S to 10°N. A longitude-height cross section of Parker's results is given in Fig. 5-2. This figure shows the basic character of the motion to be a
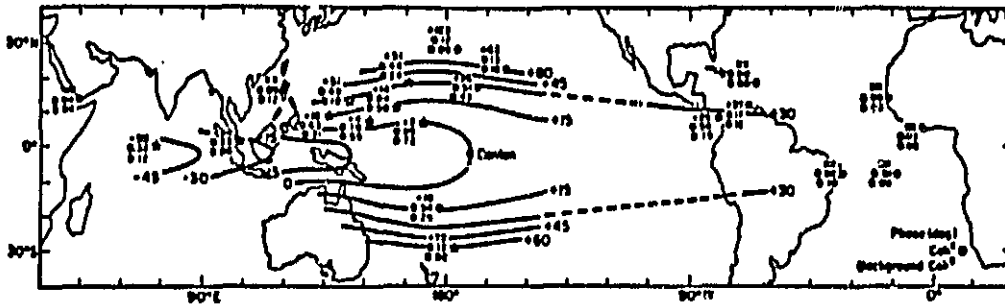
Fig. 5-1a  Mean phase angles, coherence-squares, and background coherence-squares for approximately the 36-50 day period range of cross spectra between all stations and Canton. The plotting model is given in lower right-hand corner. Positive phase angles at a station means the Canton series leads that of the station. Stations indicated by a star have coherence-squares above the background at the 95% level. Mean coherence-squares at Shemya (52°43'N, 174°6'E) and Campbell I (52°33'S, 169°9'E) (not shown) are 0.08 and 0.02, respectively. Both are below their average background coherence-squares (from Madden and Julian, 1972).
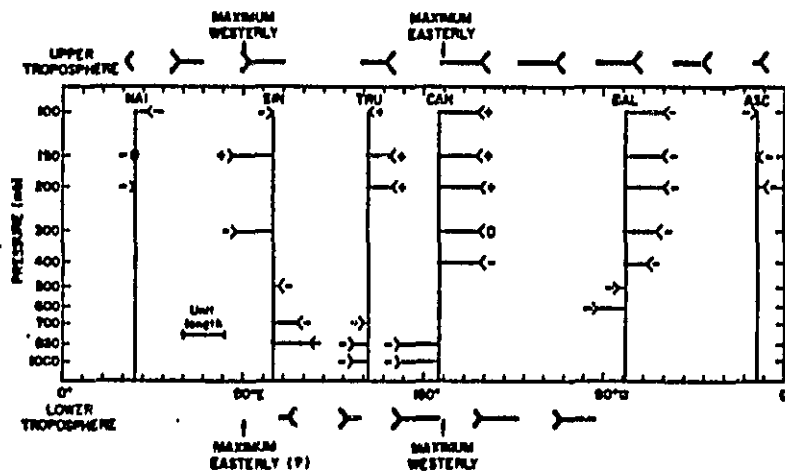


Fig. 5-1b  Zonal wind oscillation in the equatorial plane at the time when the station pressure is a maximum at Canton. The unit length represents the maximum excursion at each location. The +, -, or 0 at the tail of each wind arrow represents the sign of the instantaneous local change of the zonal wind. Arrows are plotted only at levels whose coherence squares are above their background coherence square, and whose spectra indicate a peak. Heavy arrows at the top and bottom represent a schematic of the upper and lower tropospheric wind disturbance that is consistent with the plotted wind arrows and that will satisfy the local changes if it propagates eastward (from Madden and Julian, 1972).
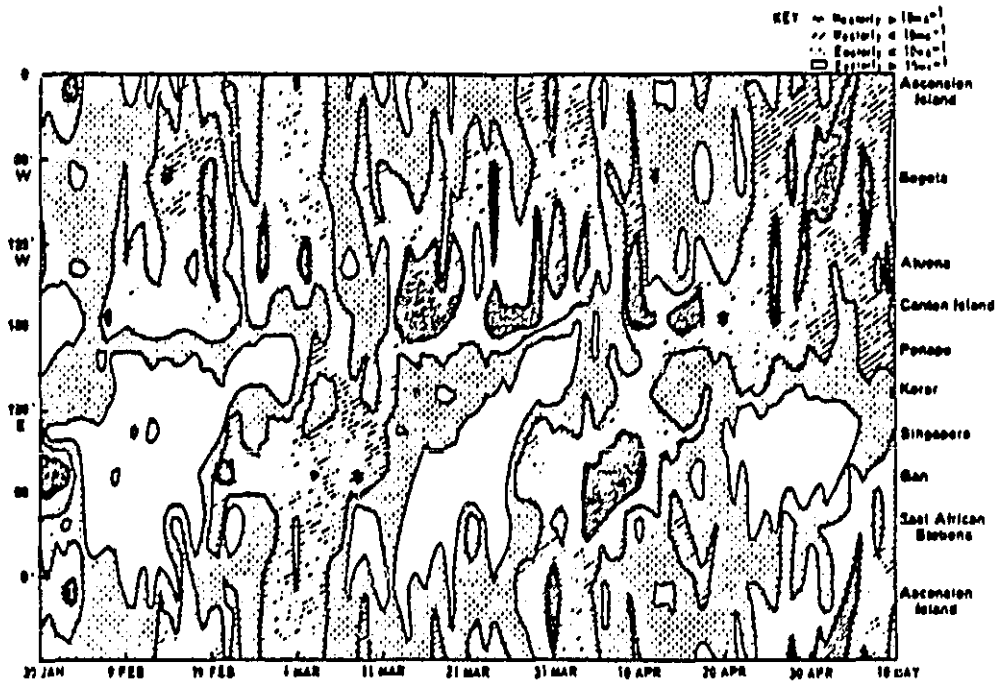
38

Fig. 5-2    Longitude-time cross section of 100 mb equatorial zonal
winds (from Parker, 1973).

mostly standing wave-like pattern with a very sharp phase transition in
the region from 120°E to the dateline. Parker proposed an explanation
for the motion in terms of an equatorial Kelvin wave. A major
difficulty with this explanation, as noted by Chang (1977), is that the
observed slow meridional propagation of the motion, particularly in the
region of the steep phase transition, is inconsistent with the observed
large vertical wavelength of the motion when examined using the Kelvin
wave dispersion relation.

Chang (1977) attempted to resolve the problem of the apparent
disagreement with the Kelvin wave dispersion relation by including the
effects of cumulus cloud momentum transport and radiative thermal
damping. One difficulty with this explanation which was pointed out by
Stevens and White (1979) is that the result is very dependent on the
values chosen for the damping coefficients. In particular the inclusion
of strong Newtonian cooling, which is necessary to slow the Kelvin
modes, is questionable in the tropical troposphere. Another concern for
any explanation involving a Doppler-shifted traveling wave is that the
mean zonal wind changes with season so that one would expect the
frequency of the oscillation to also change with season. The observa-
tions of the oscillation periods as reported by Parker (1973) and
Anderson and Rosen (1983) do not appear to show this effect. This topic
is discussed in some detail in Anderson, Stevens, and Julian (1984)
where a new analysis of the oscillation seasonality based on a 25 year
data set is presented.

Yasunari (1980) and Julian and Madden (1981) have studied varia-
tions in tropical cloud cover and have confirmed the Madden and Julian
hypothesis that the eastward propagating surface lows are associated
with enhanced cumulus convection.

Langley et al. (1981) studied the relationship between the total atmospheric relative angular momentum and the rotation rate of the Earth. These quantities are related by the requirement that the total angular momentum of the earth-atmosphere system be conserved when solar and lunar tidal effects are accounted for. Langley et al. found that there were coherent quasi-periodic fluctuations in both quantities with periods in the 40-50 day range. Anderson and Rosen (1983) showed that these variations were due to the zonally symmetric component of the tropical motions. Their results, which are depicted in Fig. 5-3, show a spatial structure which has its maximum amplitude in equatorially symmetric maxima located at approximately 20°N and 20°S. The zonally symmetric motions propagate poleward and downward in phase from a phase center located in the equatorial upper troposphere. The observations of Anderson and Rosen also indicated the presence of a northern hemisphere mid-latitude component to the oscillation. This component, which also appears in a nonsymmetric analysis by Weickman (1983), is probably the response of the mid-latitude climate to changes in the tropical forcing.

The observations of a zonally symmetric oscillation raise the possibility that the basic source of the 40-50 day period may result from the symmetric rather than the wavenumber 1 component. This hypothesis was offered support by Goswami and Shukla (1984) who report the results of a study using a zonally symmetric version of the GLAS general circulation model. They noted a tendency for the model circulation to oscillate with periods on the order of a month; however, the oscillations occurred in their model only when an explicit water budget and cumulus heating parameterization were included.
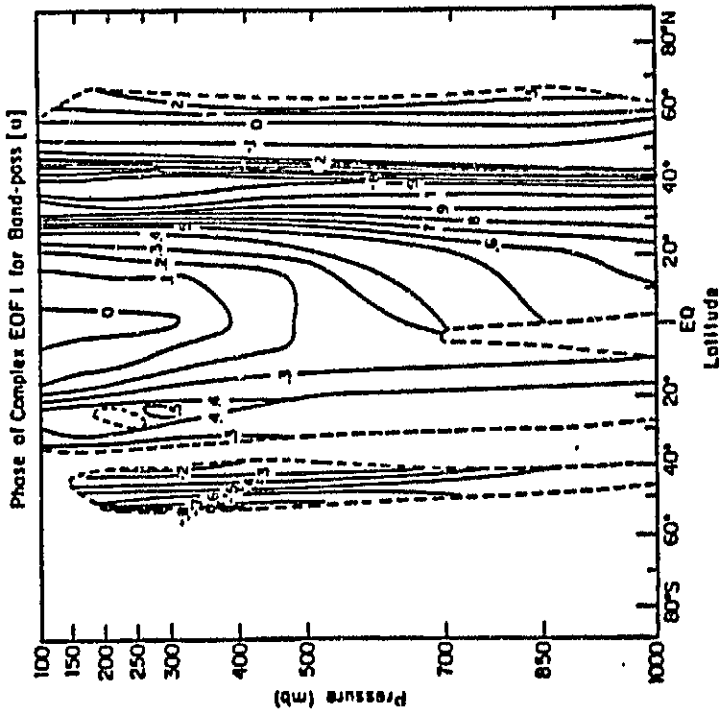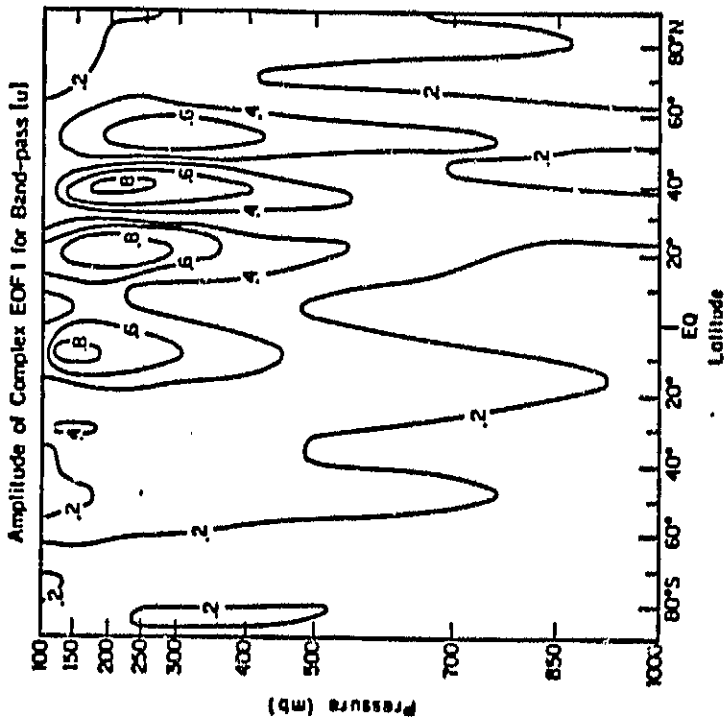
Fig. 5-3   Phase-amplitude analysis of the observed oscillation latitude-height structure (from Anderson and Rosen, 1983).   Phase convention is from -1 to 1 with propagation direction from smaller to larger.

One of the critical questions in the explanation of the oscillation now appears to be the relationship between and the relative roles of the wavenumber 0 and nonsymmetric motions in the oscillation. In a very recent paper, Yamagata and Hayashi (1984) report the results of using a simplified shallow water model, similar to the one developed by Gill (1980), to examine the effects of locally forcing an equatorial atmosphere with a heat source which has a 40 day periodicity. The results of this study show that the principal features of the observed nonsymmetric components of the oscillation can be explained as a response to local forcing in the maritime continent region. Their analysis did not indicate any source for the time scale of the motion.

In this work the possibility that the time scale for the motion comes from symmetric processes is further examined. In particular, various calculations are made to determine the effects of a basic state consisting of a simple "Hadley" type circulation on the large scale tropical motions. It is shown in Chapter 3 of Anderson (1984) that the inclusion of these effects results in the formation of a new time scale for the dynamics which arises from the advection of perturbation quantities by the Hadley cell mass circulation. The existence of this time scale results in a new class of slowly oscillating linear normal modes, some of which have many similarities with the observed oscillation. These modes are discussed in some detail in Section 5.2 below.

The forced symmetric and nonsymmetric response of the atmosphere are discussed in Chapter 4 of Anderson (1984) and in Anderson and Stevens (1985) where the resting basic state shallow water analysis of Yamagata and Hayashi (1984) is extended to include the effects of a more realistic basic state. The purpose of this component is to examine the

possibility that the nonsymmetric motion may result from the modulation of the strong western Pacific convection by the symmetric mode.

The results of the dynamical calculations are then compared with the available observational data to determine the plausibility for this explanation of the oscillation. In particular, comparison is made in Anderson, Stevens, and Julian (1984) with the symmetric study of Anderson and Rosen (1983) and the recent three dimensional study of the FGGE Summer MONEX by Murakami et al. (1983).

## 5.2    A new class of slowly oscillating symmetric modes in the tropical troposphere

A primary result of our model investigation is the identification of a new class of slowly oscillating modes in the tropical troposphere. These modes appear only if a Hadley cell circulation in the meridional plane is included as part of the basic state.

To demonstrate this phenomenon, we show in Figure 5-4 the complex frequencies of model normal modes with a resting basic state. The symmetric model includes some dissipation: Therefore all the modes decay with time. The rapidly oscillating modes on the right correspond to the symmetric (k=0), high-frequency gravity modes shown on Matsuno's (1966) dispersion diagram, reproduced in Fig. 5-5. The "column" of essentially zero frequency modes on the left of Fig. 5-4 represent the exactly geostrophic modes at zero frequency on Matsuno's diagram (5-5). Note the clean separation of the eigenvalues between exponentially decaying thermal wind modes and fast oscillating gravity modes.

Next we include the effects of a Hadley cell basic state, which is derived from a nonlinear calculation. Figs. 5-6a through d display the zonal wind, meridional wind, potential temperature, and vertical
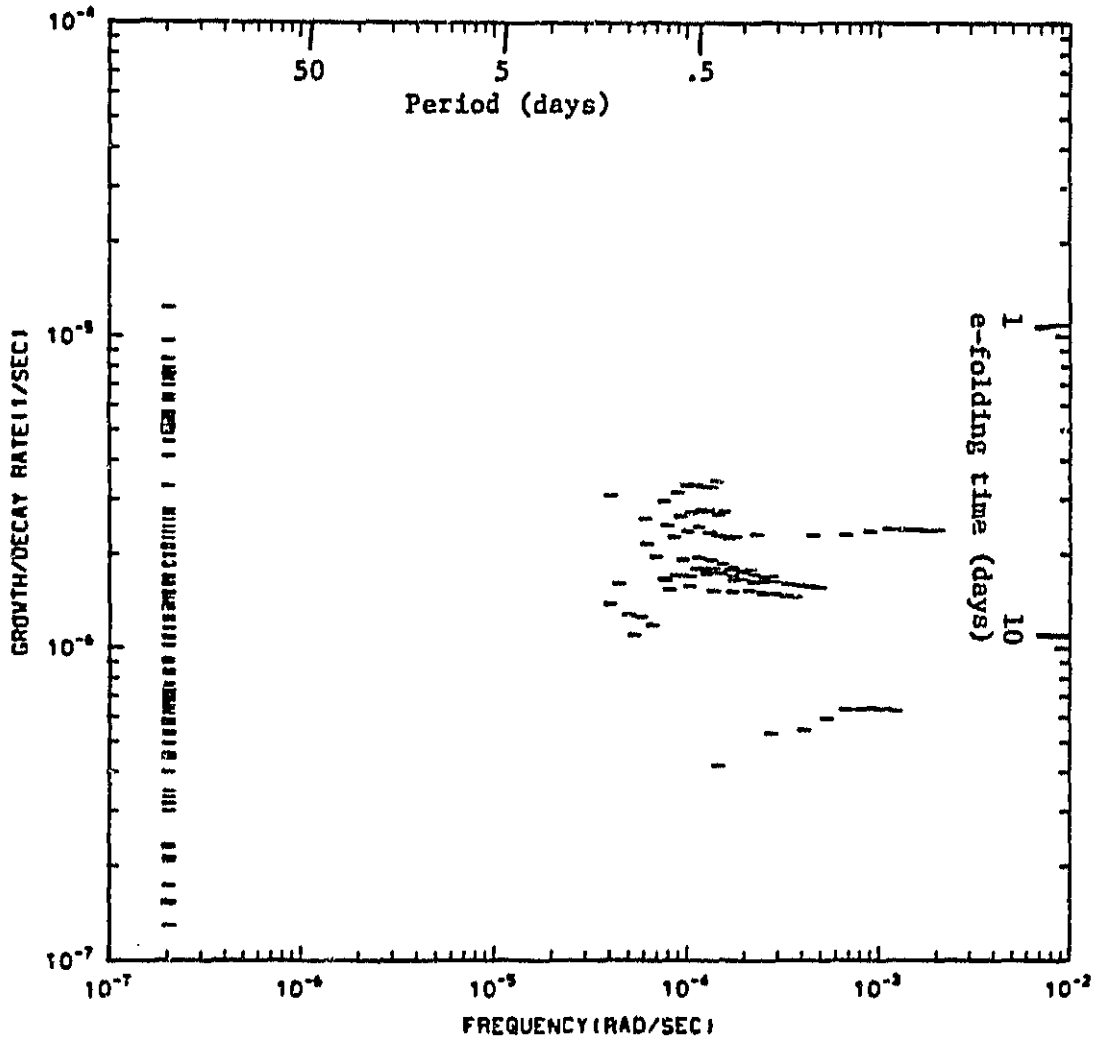
Fig. 5-4   Model normal mode complex frequencies for resting basic
state.   Modes with frequency <2. $10^{-7}$ rad/sec are
plotted there.   Damped modes are plotted as -, growing
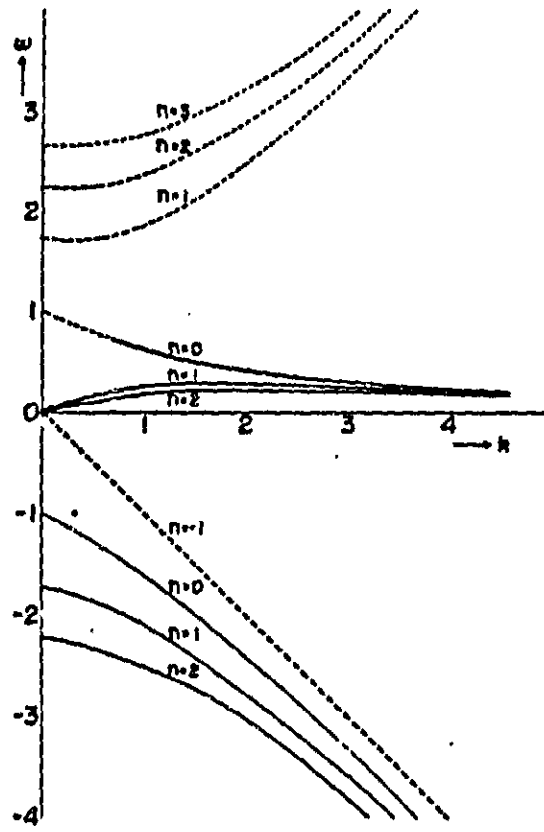modes as +.

45



Fig. 5-5   Dispersion diagram for one vertical mode of an equatorial atmosphere.   Thin solid line:   eastward propagating inertia-gravity waves.   Thin dashed line:   westward propagating inertia-gravity waves.   Thick solid line:   Rossby (quasi-geostrophic) waves.   Thick dashed line:   The Kelvin wave (from Matsuno, 1966).
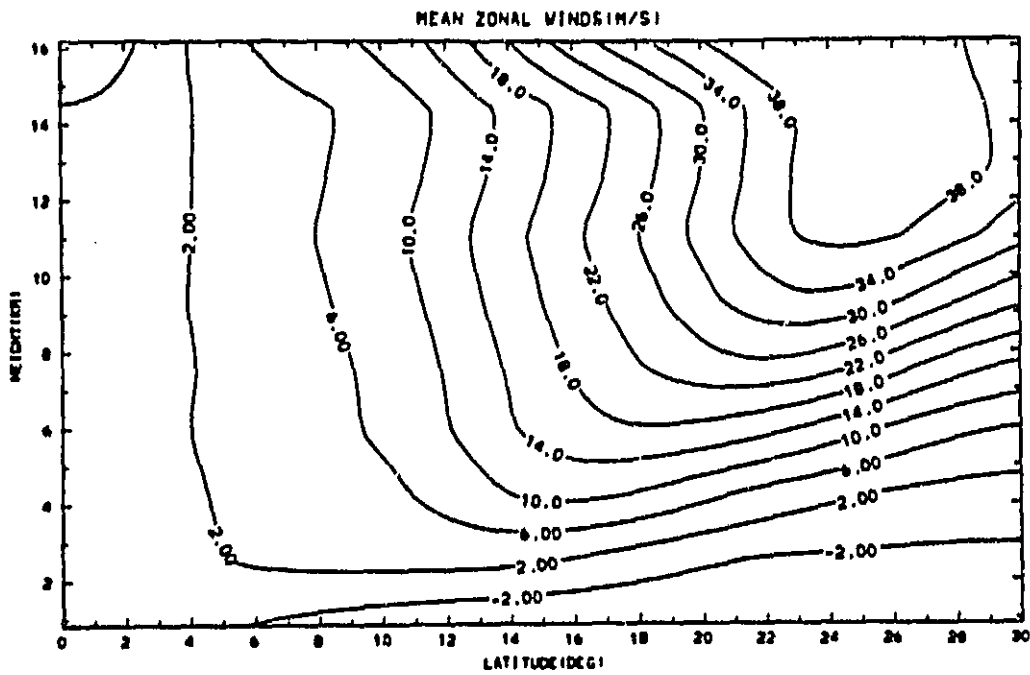
MEAN ZONAL WINDS(M/S)

Fig. 5-6a    Basic state u=wind field for $N_z$=10, 10 meridional wave-numbers.



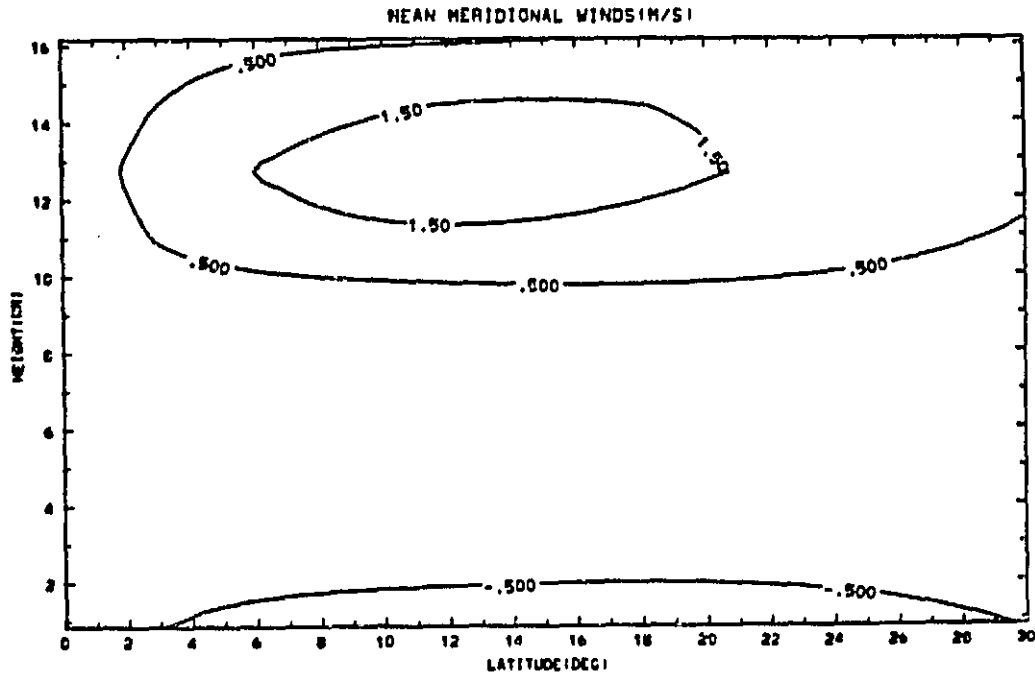MEAN MERIDIONAL WINDS(M/S)

Fig. 5-6b    Basic state v-wind field for $N_z$=10, 10 meridional wave-numbers.

**POT. TEMP. DEPARTUE FROM REFERENCE(K)**
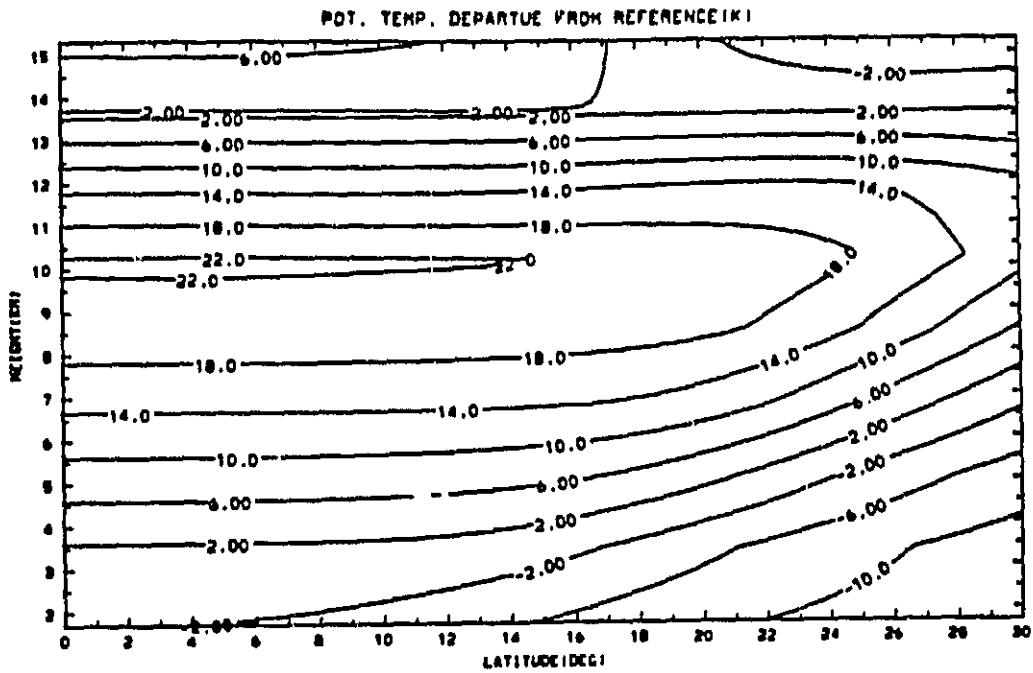


Fig. 5-6c    Basic state potential temperature field for $N_z$=10, 10 meridional wavenumbers.
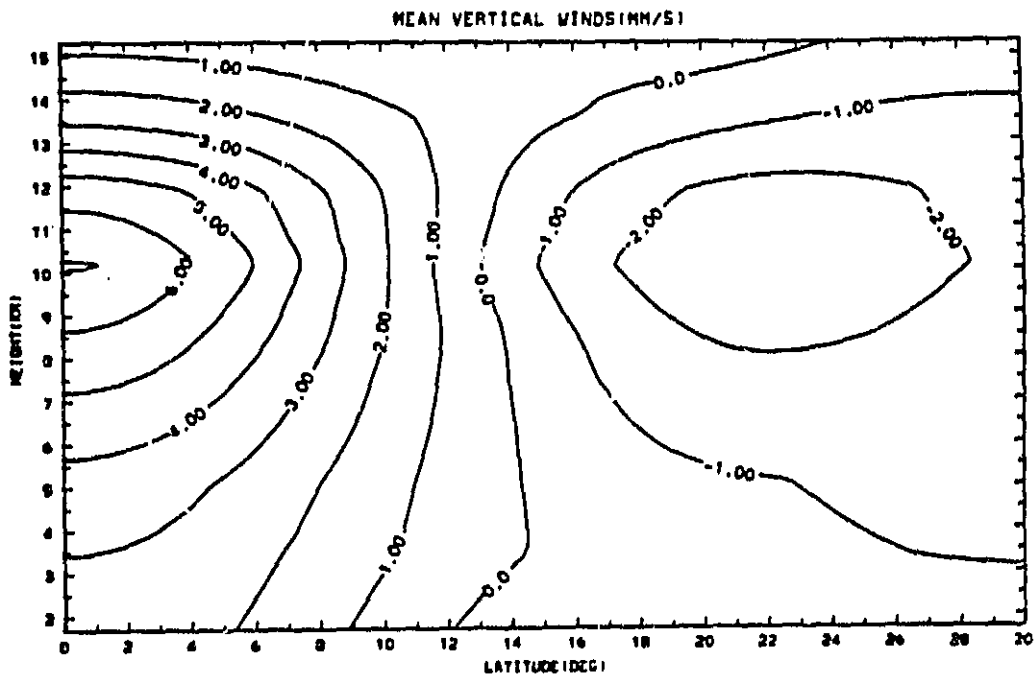
**MEAN VERTICAL WINDS(MM/S)**



Fig. 5-6d    Basic state w-wind field for $N_z$=10, 10 meridional wavenumbers.

velocity fields for this Hadley cell. The results, plotted in Fig. 5-7, show that now there are a set of slow oscillatory modes in addition to the gravity modes. One of those modes with a period of ~52 days has a very slow decay time and is circled on the plot. The u-field structure of this mode is presented as Fig. 5-8 and is in good agreement with prognostic runs, reported in Anderson (1984), which clearly show the poleward propagation in phase. The v-field is approximately two orders of magnitude smaller than the u-field and the θ-field is in thermal wind balance with the u-winds. In Fig. 5-9 we present the mode structure when $\bar{M}_c$ (the basic state cloud mass flux in the cumulus friction terms) is set to baseline value and $M_c'=Q'=0$. For this case there are a set of modes with periods from ~30 to ~50 days which decay at approximately the same rate. This bredth in frequency is in agreement with the broader frequency response seen in the prognostic runs. Finally, we add the representation for perturbation heating $Q'$ and $M_c'$ given in the Stevens-Lindzen parameterization scheme to produce the results which are shown in Fig. 5-10. In this set there are now some fast growing unstable modes which are marked with boxes. These modes are fast gravity waves which are destabilized by the convection. The slow modes on the other hand are essentially unchanged.

The inability of the current model to allow the slow modes to interact with the latent heating field is somewhat disappointing due to the strong evidence for such an association in the observed oscillation. This lack of response by the model slow modes is not too surprising since the Stevens-Lindzen scheme links latent heat release to boundary layer convergence and the model slow modes are essentially non-divergent. A more complete cumulus parameterization scheme would have
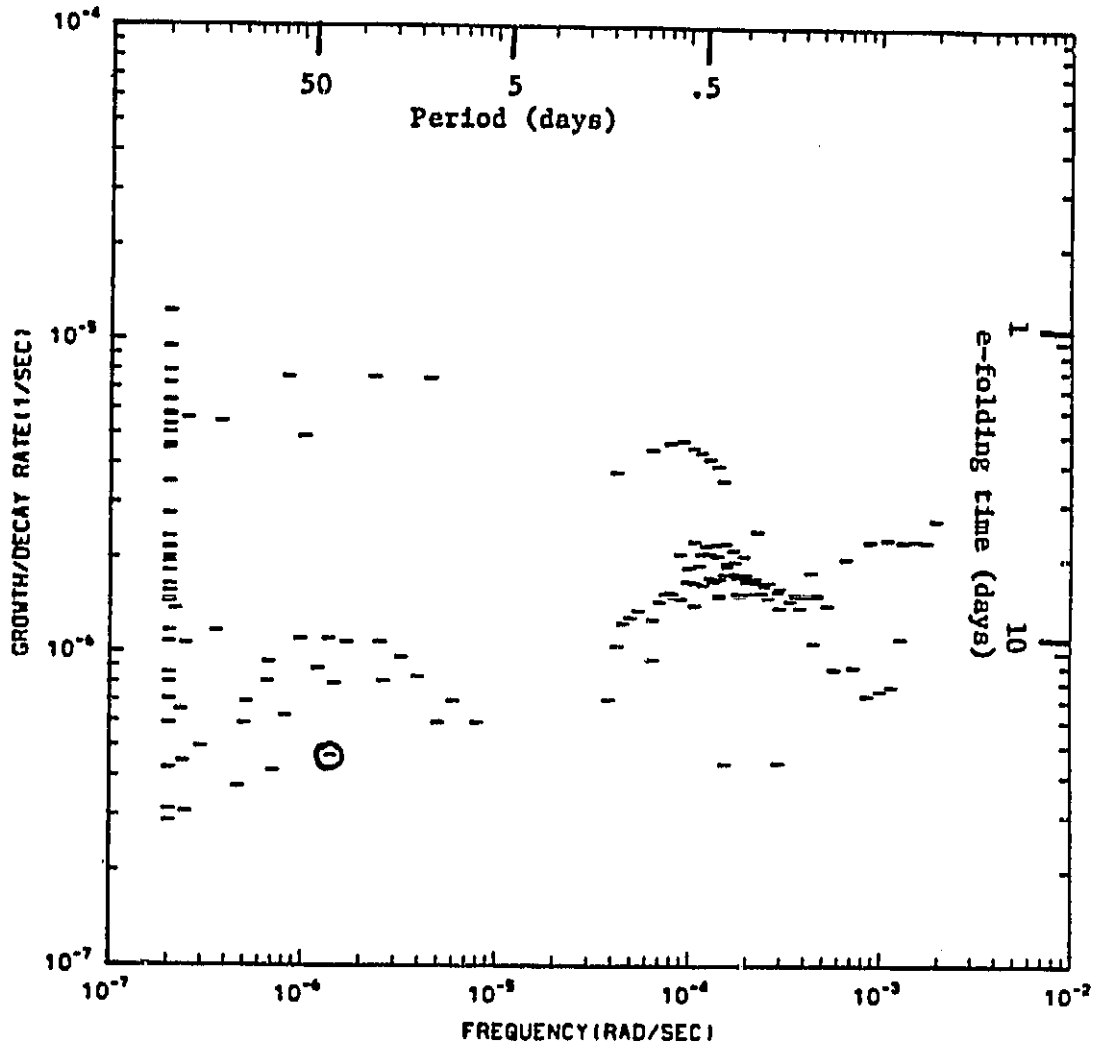
Fig. 5-7    Like Fig.  5-4  for parameters like run 3.

$\omega t = 0°$
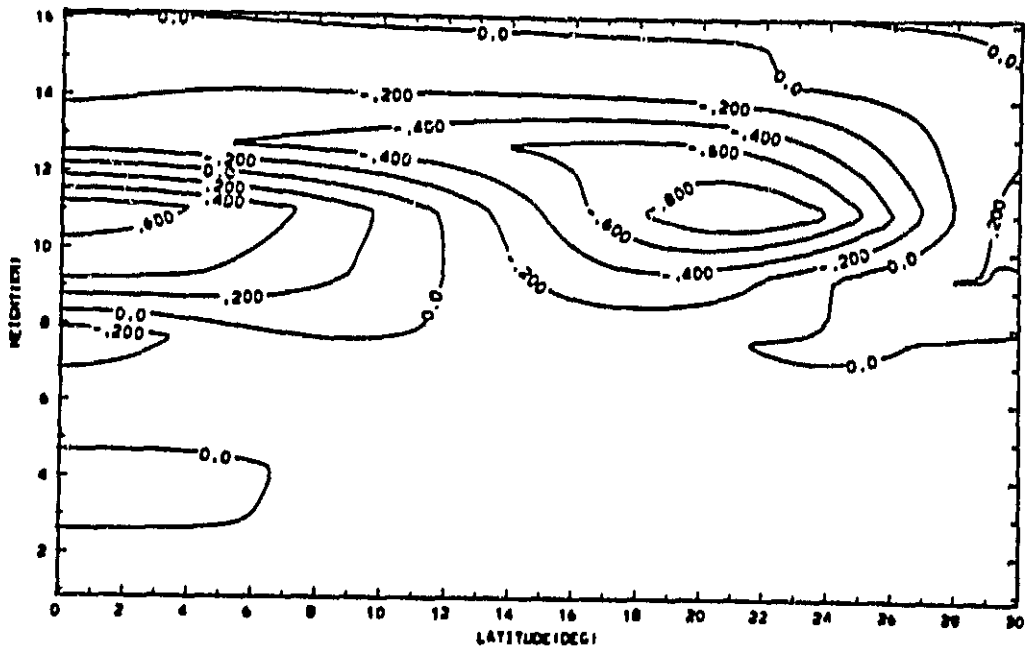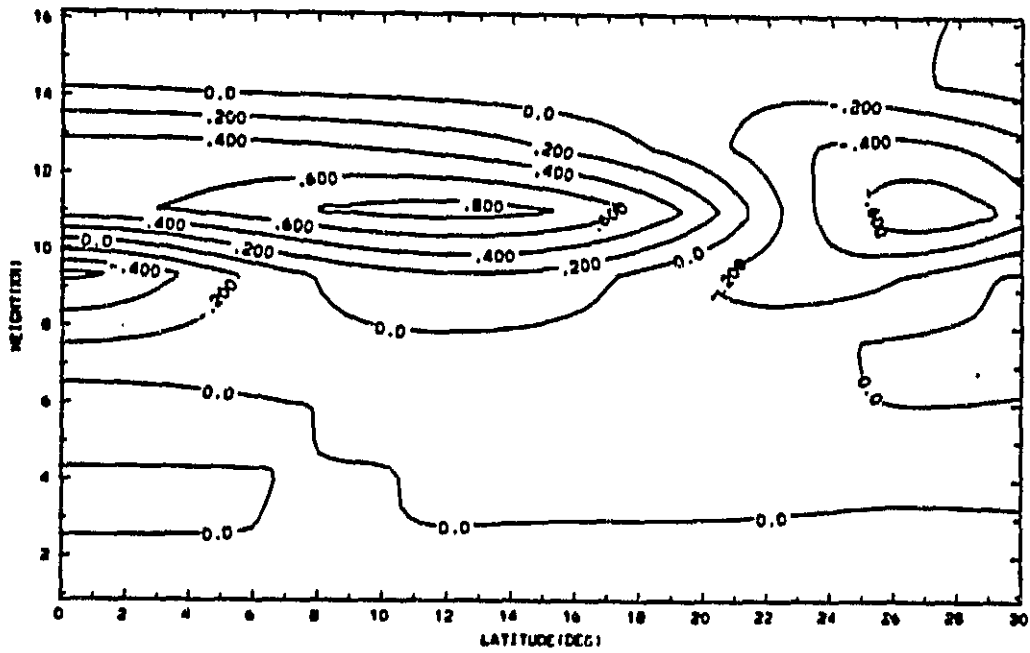


$\omega t = 90°$

Fig. 5-8    Spatial u-wind structure of mode which is circled on
            Fig. 5-7

51
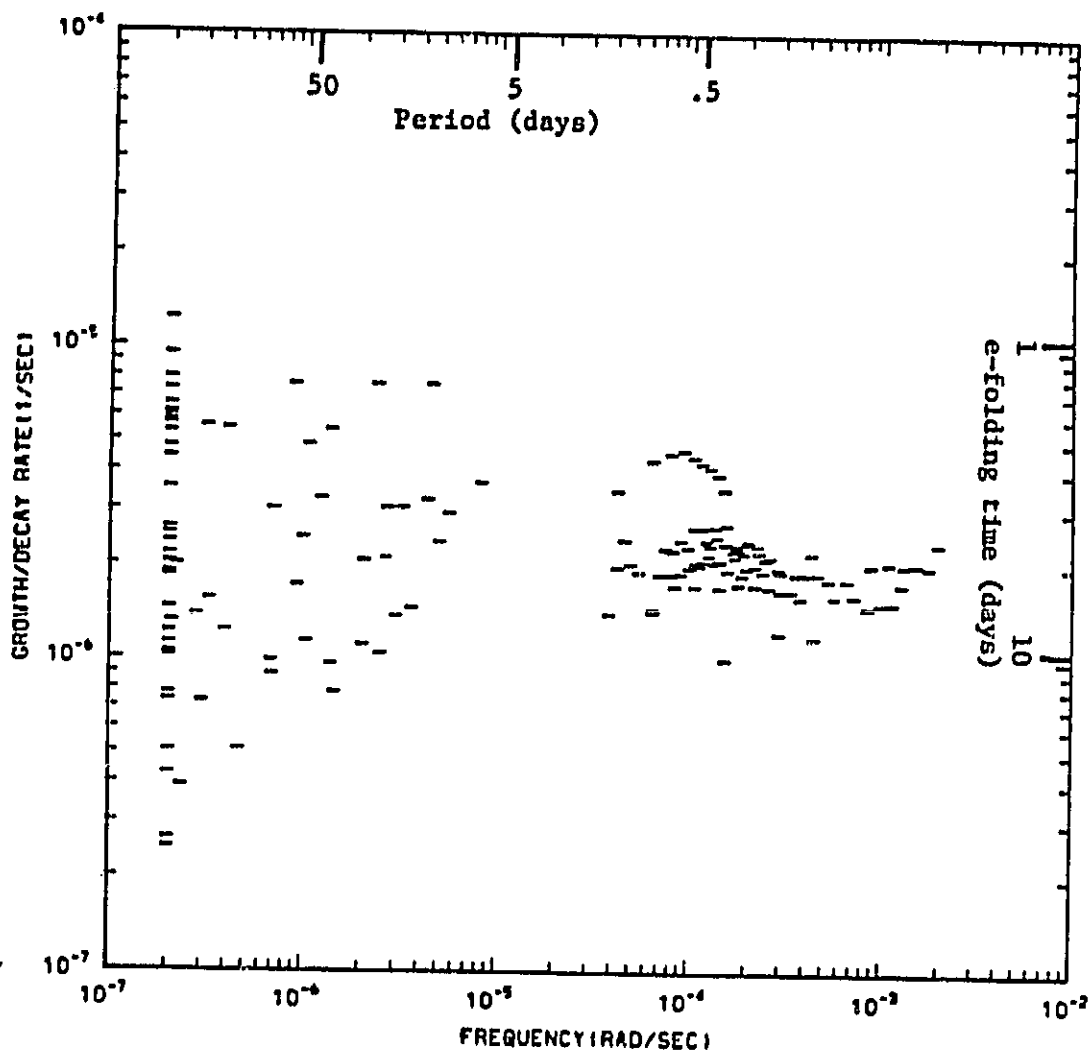
Fig. 5-9    Like Fig. 5-4   for baseline model.
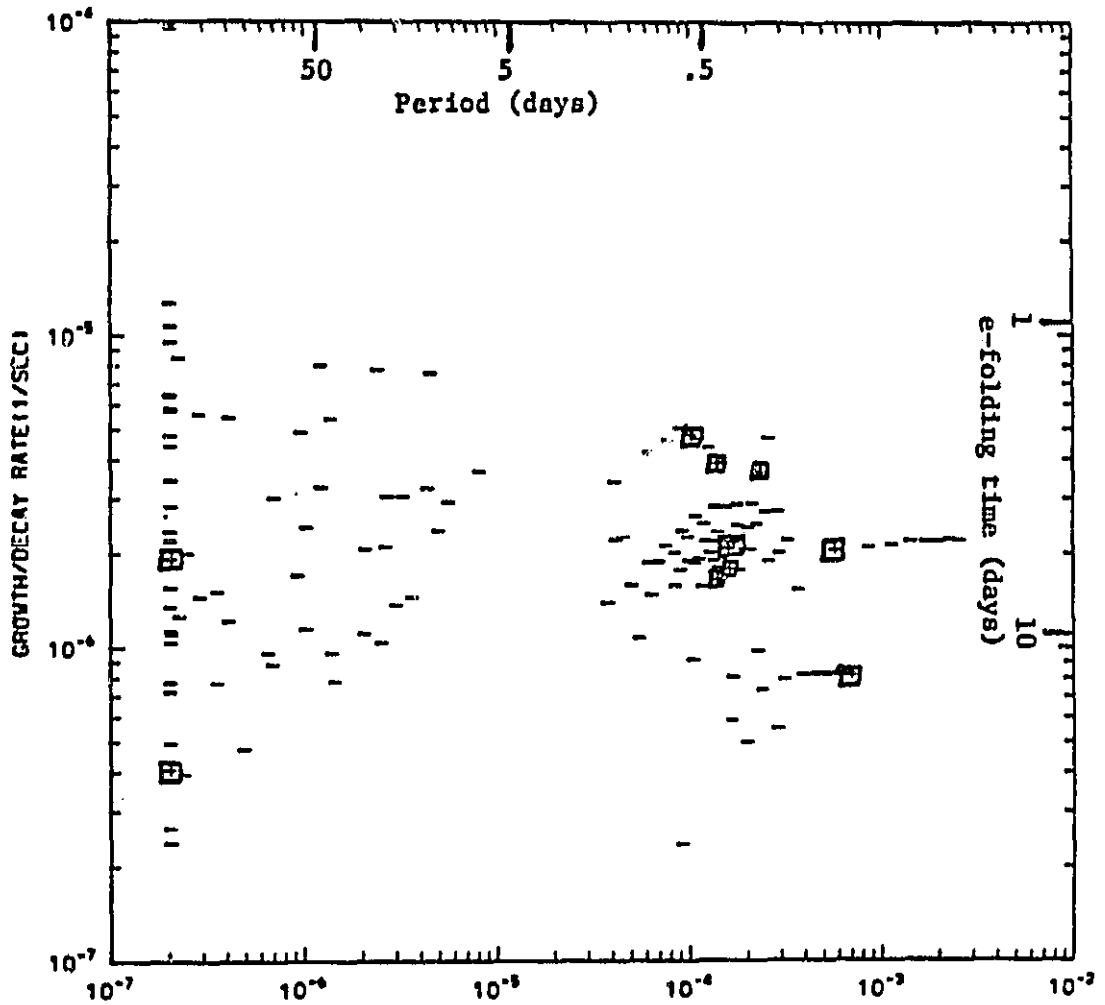
Fig. 5-10    Like  Fig.  5-4    for  baseline  model  with  Stevens-Lindzen
    cumulus  parameterization.

to take into account the dependence of the convection on changes in the static stability and the effect of the zonal circulation on the tropical wave disturbances in which the clouds themselves are embedded. For example, Goswami and Shukla (1984) determined that slow oscillations in the GLAS GCM were related to changes in moist convective instability in the tropics. The simple cumulus parameterization used here relates convection to horizontal convergence of moisture but not directly to changes in thermodynamic properties of the atmosphere such as convective instability.

In summary, the inclusion of a basic state Hadley circulation in the model creates a new class of slow oscillating modes which are capable of producing response peaks in the 40-50 day range from forcing which is random in time. The model however fails to couple the slow modes to cumulus heating when a simple moisture convergence cumulus parameterization is used.

## 5.3 Discussion of results and comparison with observations

In the introduction we discussed the observational history of the 40-50 day oscillation. It is perhaps surprising that a phenomenon which exhibits a near regular periodicity during all seasons and affects nearly every tropical meteorological parameter has eluded explanation for so long.

The first mechanism proposed as the basis of the oscillation time scale was presented by Chang (1977). Chang attempted to show that a possible cause of the time scale could be the time it takes a zonal wavenumber 1 Kelvin wave to travel around the planet when account had been taken of the effects of Doppler shifting by the mean zonal wind and the frictional effects of cumulus clouds. One consequence of this

mechanism is that one would expect this time scale to change with season as the mean winds vary with the semiannual and annual cycles. In Anderson, Stevens and Julian (1984) we present an analysis of the seasonal variation of the oscillation period and find it to change little, if any, with season. This small variability would seem to cast doubt on the viability of this explanation for the period, although the mechanism which Chang proposed may well explain the eastward propagation of the observed motion if the oscillation period is externally forced.

Webster (1983) has proposed a mechanism by which fluctuations on this time scale in a simple zonally symmetric monsoon model result from the storage times for moisture in the soil. Webster does not say in the paper if he feels that this mechanism could be responsible for the oscillation at times when there is not an active monsoon circulation and it seems unlikely that this effect could explain the phenomenon during the seasons when most of the precipitation occurs in oceanic areas.

In this work we present a third hypothesis, namely that the oscillation time scale results from the advective time scale associated with a basic state Hadley circulation. We investigate the effects of the Hadley circulation on equatorial wave modes in Chapter 3 of Anderson (1984) and find that the thermal wind modes of the resting basic state now appear as modes which oscillate slowly. We also find that the modes which are the least damped tend to have periods in the 30-60 day range yielding a response spectrum to white noise forcing which has an enhanced amplitude at these frequencies. Comparisons with the observed spectra which appear in Chapter 5 (of Anderson (1984) still however show that the observed oscillation spectral peak is sharper than that which can be achieved with reasonable values of dissipation. To generate a

peak as narrow as the observed spectra we would need a mode which is nearly neutral, probably requiring some energy source other than random forcing.

The presence of the response peak in the modes at periods of approximately 50 days can be explained in the relationship between the size and frequency of the "advective" modes. In general, approximately geostrophic modes which have lower frequencies tend to lose less energy to gravity waves when thermally forced than faster motions. When the advective effects are considered, however, the slower motions are forced to have large spatial scales. When the requirement that the mode contain some thermal gradient inside the domain is imposed so that there will be an associated wind field, a low frequency limit is placed on the modes with u-wind fields at ~50 day periods. These modes have a single wind maximum between the equator and the poleward boundary. The poleward boundary is very dissipative, simulating the effects of the mid-latitude cyclones. The prognostic runs presented in Chapter 3 of Anderson (1984) show that the least damped model motions tend to exhibit phase propagation of the zonal wind which is poleward and downward in agreement with the phase-amplitude eigenvector analysis of Anderson and Rosen (1983) This observational analysis is described in Fig. 5-3 of the Introduction.

One rather unsatisfying result of the calculation is that the model slow modes, due to their very small divergence, do not interact with cumulus cloud latent heat release as parameterized by a simple moisture convergence scheme (Stevens and Lindzen, 1978). This negative result seems to indicate the necessity of a more elaborate parameterization,

which is difficult to design in a strictly linear context, in order to appropriately describe and model the interaction between the slow modes and deep convection.

The inability of the model to couple the dynamical slow modes to cumulus convection represents a significant gap in an explanation of the 40-50 day oscillation. Simulation of the narrowness of the observed spectra requires either a coherent energy source or smaller than expected frictional dissipation. The energy source is probably supplied by a modulation of the tropical deep convection. This coupling may involve dynamical effects which we have not included - such as the effects of variations of tropical stability on the clouds - or it may result from physical processes such as the storage of soil moisture as described by Webster (1983).

In Anderson and Stevens (1985) we study the response of a tropical atmosphere to 40-50 day period thermal forcing with a number of models. The shallow water calculation of Yamagata and Hayashi (1984) is extended to a more general basic state and seems to give reasonably good agreement with observations for the oscillation structure in the tropical Pacific. The model indicates a geopotential response which is relatively smooth throughout the region and a u-wind field which exhibits a phase jump in the heating region at low latitudes. In Fig. 5-1 we presented the results of an analysis of the surface pressure and the zonal wind fields by Madden and Julian (1972) which depicts these same features. These results indicate that the non-zonally symmetric part of the tropical u-response could be due to a spatially localized maximum in the heating field which could be modulated in some way by the zonally symmetric motions.

When the effects of the Hadley cell basic state are included in the forced calculation, the model shows a maximum u-wind response in the subtropical region east of the heating which propagates poleward and eastward. In Fig. 5-11 we present an analysis from Murakami et al. (1983) of the 40-day period, 200 mb zonal wind variations during the FGGE summer MONEX period. This analysis shows a zonal wind maximum in the Northern Hemisphere eastern Pacific subtropics with a well-defined eastward phase propagation, in agreement with the model results.

Anderson and Stevens (1985) also presents the results of the zonally symmetric forced response for the Hadley cell basic state. This model response shows the formation of a wind anomaly which originates at the surface in the equatorial regions and then propagates poleward and eventually downward under the influence of the Hadley circulation. See Fig. 5-12. This representation is in reasonable agreement with the Anderson and Rosen results for the region poleward of 15° North; however, the Anderson and Rosen results do not show the upward vertical propagation of the equatorial anomaly or the strong lower tropospheric winds. Observations by Murakami et al. (1983) of a partial zonal average taken over the monsoon region (60°E to 160°E), which is reproduced as Fig. 5-13, show a sequence almost exactly the same as the model forced motion during the summer monsoon. These results suggest that this feature of the oscillation may only occur in the regions where latent heat release is occurring.

An extremely interesting result of the forced symmetric calculation is that at the time of maximum heating the perturbation temperature field is such that it will tend to destabilize the troposphere. Thus the possibility exists that this destabilization may be the mechanism
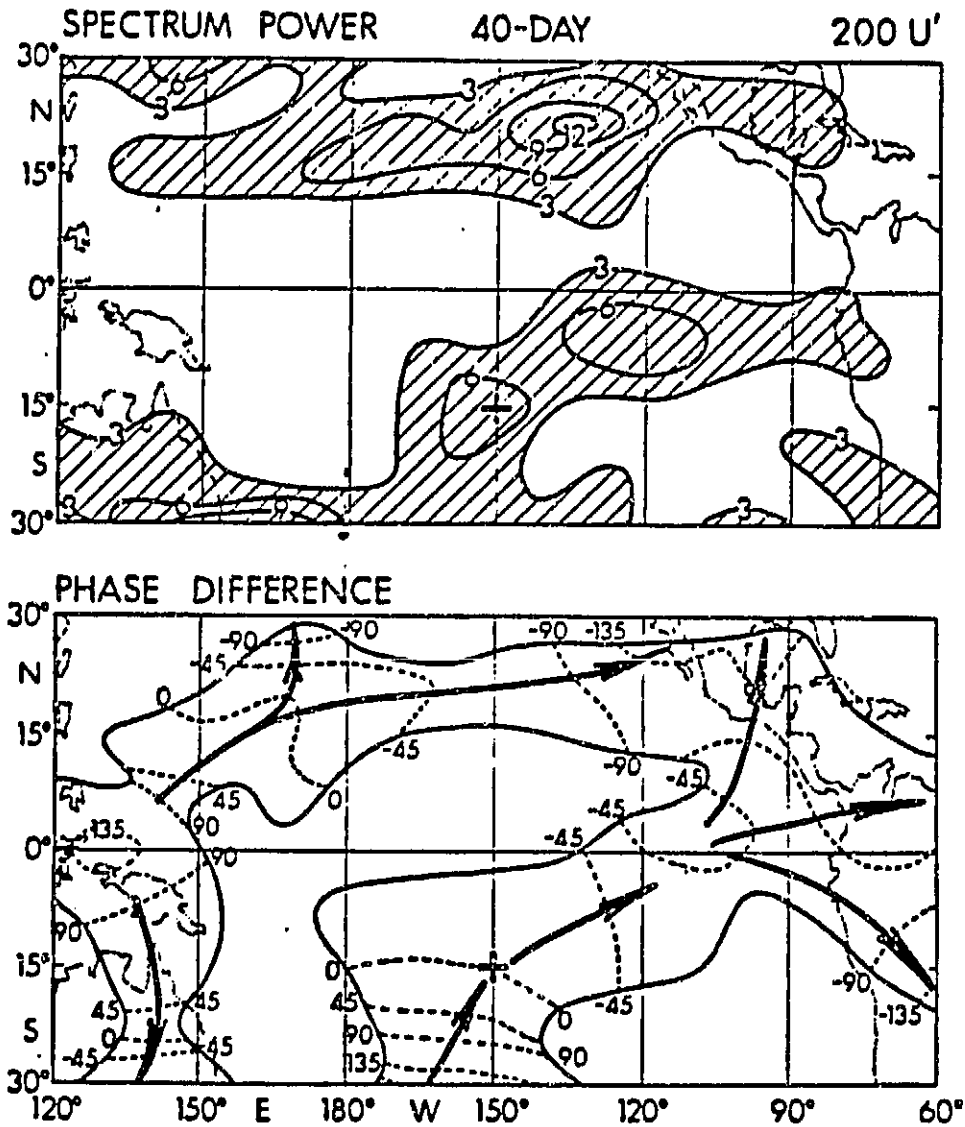
Fig. 5-11   Observed oscillation phase and amplitude for 200 mb u-winds (from Murakami et al., 1983).
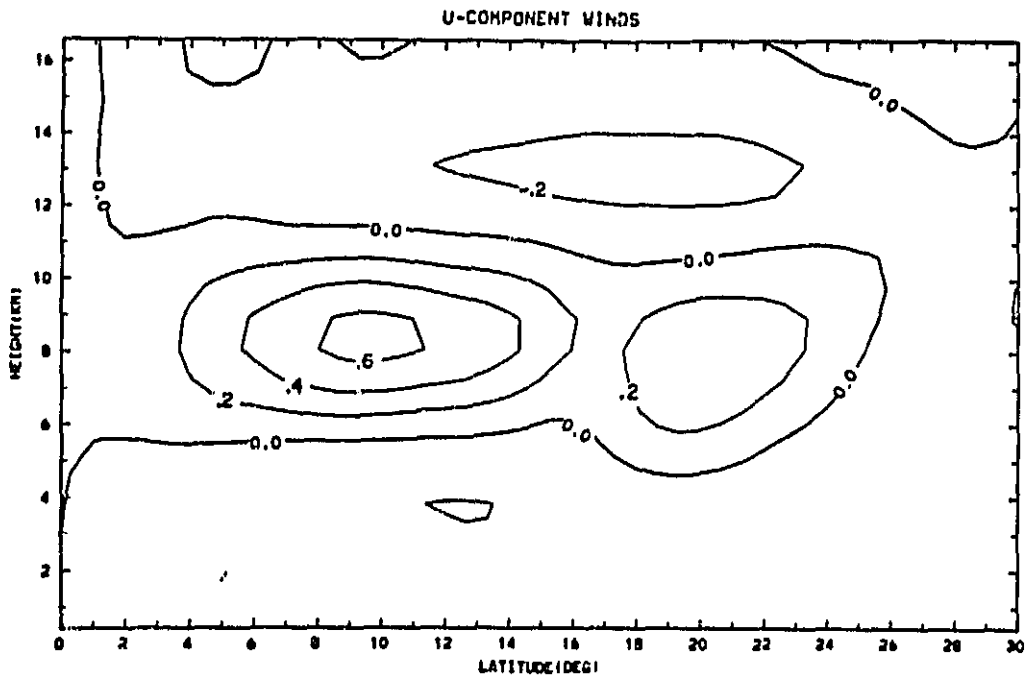
Fig. 5-12a    Wavenumber 0 response at ωt = -45 deg for Hadley cell
calculation.
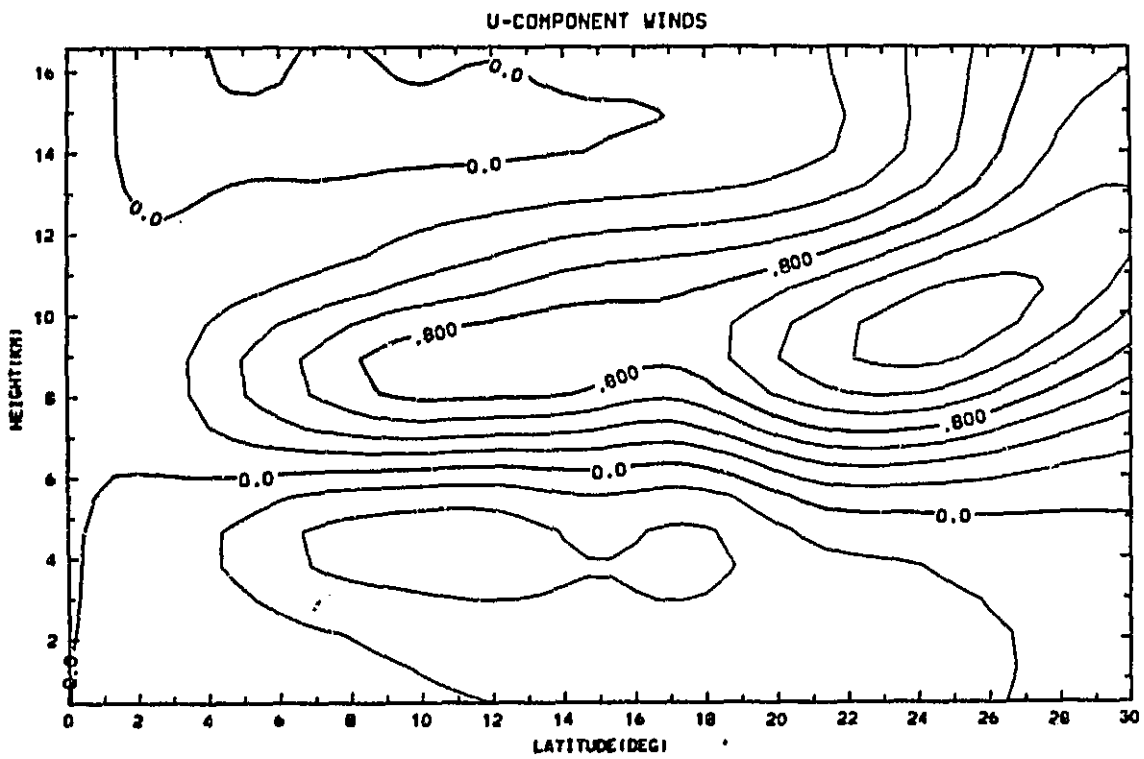


Fig. 5-12b    Wavenumber 0 response at ωt = 0 for Hadley cell
calculation.
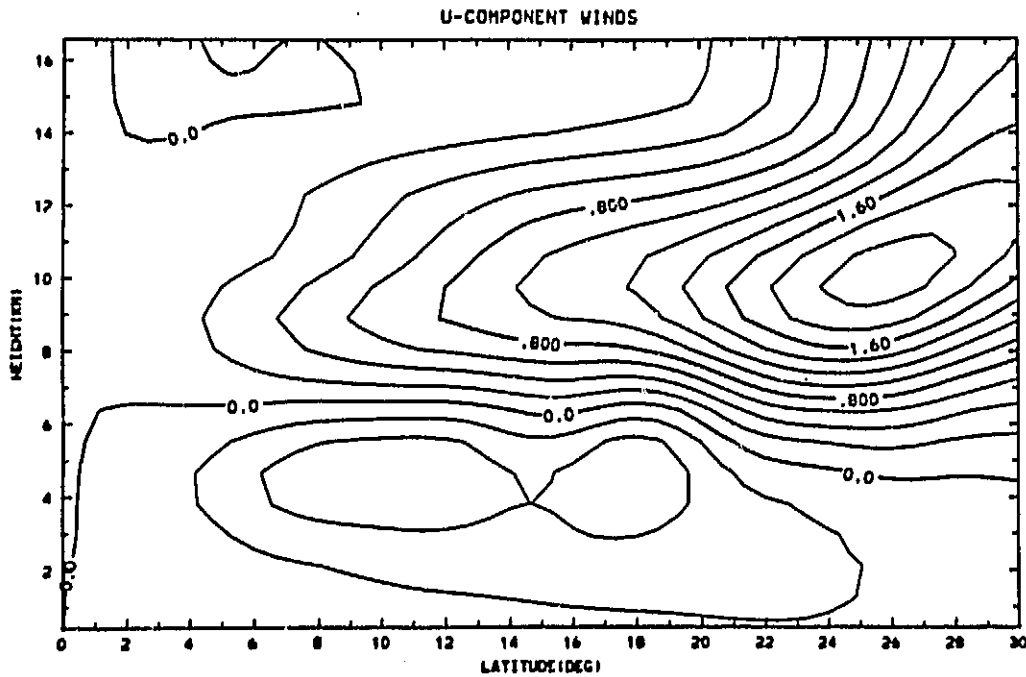
Fig. 5-12c    Wavenumber 0 response at ωt = 45 deg for Hadley cell
calculation.



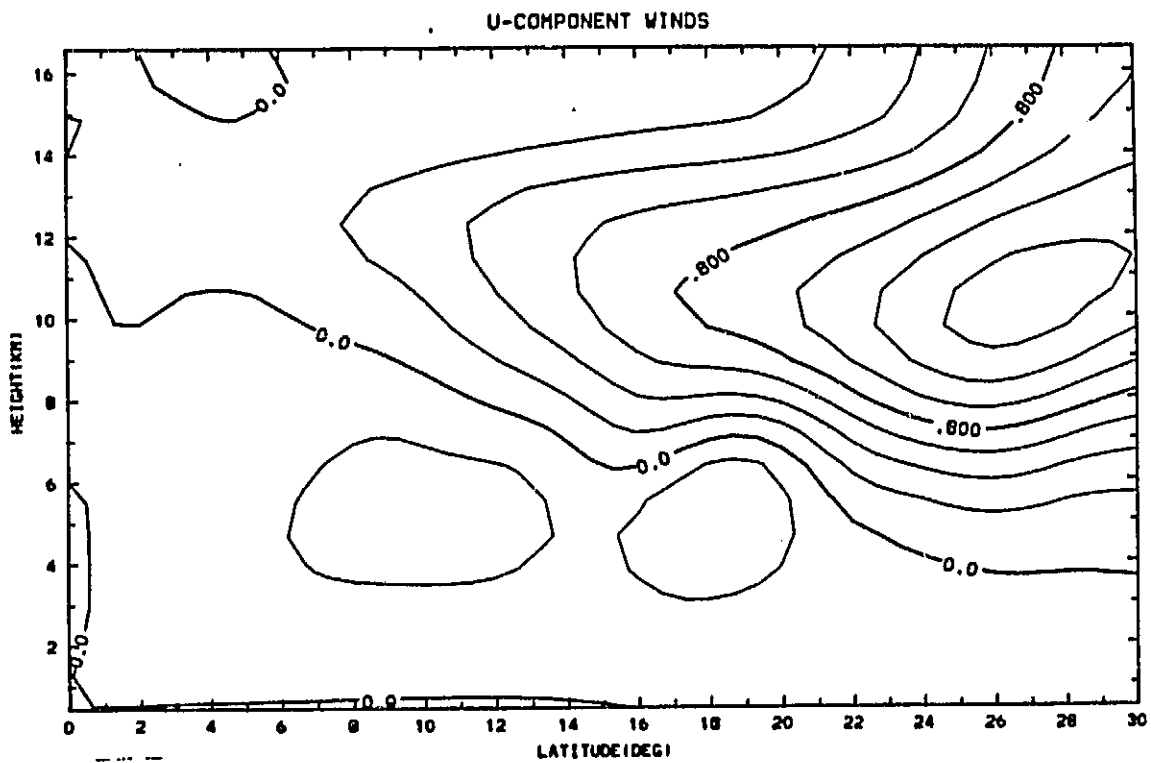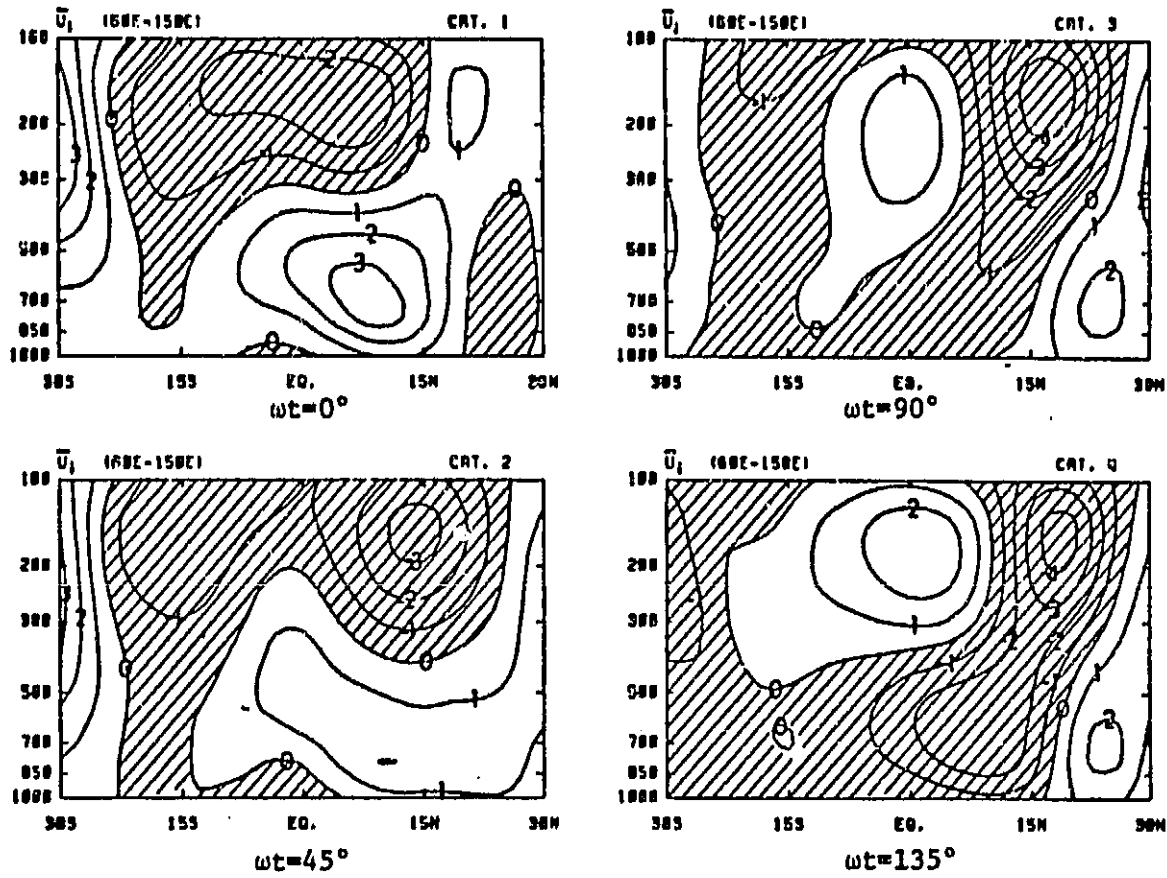Fig. 5-12d    Wavnumber 0 response at ωt = 90 deg for Hadley cell
calculation.

Fig. 5-13  Latitude-height structure of partial zonal average (60°E to 160°E) u-wind field (from Murakami et al, 1983).

which gives rise to the increased convective heating and provides the oscillation energy source. This effect is very difficult to parameterize in a purely linear model; however, in a nonlinear, zonally symmetric model which uses a convective adjustment cumulus scheme which is sensitive to the local stability, Goswami and Shukla (1984) report similar low frequency oscillations which appear only when moisture is included.

In Anderson, Stevens and Julian (1984) we present an analysis of the "seasonality" of the observed oscillation. One result, which is mentioned above, is that the oscillation frequency appears to vary little, if any, with season. A second result is that the oscillation measured at Truk is certainly a year-round phenomenon, and there is no evidence that the oscillation is stronger during the monsoon periods; in fact the oscillation amplitudes appear to be maximum during the equinoxial periods. Based on their study of the FGGE summer monsoon experiment, Murakami et al. (1983) state that "the monsoon region represents the major energy source for 40-50 day perturbations". The observations of the temporal variation indicate that while this may be true during the summer monsoon, the oscillation must have some other energy source during the seasons that the monsoon is not active. The results of this study suggest that the oscillation may be a natural variation of a direct Hadley-type circulation. During an active monsoon, when that region represents the major source of heating, the motion could be due to a modulation of a monsoon circulation. When the monsoons are inactive this variation may result from a modulation of the other Hadley cell regions, particularly the west Pacific ITCZ.

In this study we have limited ourselves to the very simplest possible model which contains the effects of a Hadley cell type mean circulation. Future work should involve considering the case of a Hadley cell which is not equatorially symmetric and the effects of the non-zonally symmetric "Walker" and monsoon circulations on the perturbation modes. In addition a full understanding of the energy source for the 40-50 day motions will not be possible until a better representation of the interactions between the large scale motions and deep convection is included, presumably through the solution of a nonlinear system.

## 6. References

Anderson, J.R., and R.D. Rosen, 1983: The latitude-height structure of 40-50 day variations in atmospheric angular momentum. J. Atmos. Sci., 40, 1584-1591.

Anderson, J.R., 1984: Slow motions in the tropical troposphere. Atmospheric Science Paper No. 381. 144 pp; Colorado State University, Fort Collins, Co 80523

Anderson, J.R, D.E. Stevens and P.R. Julian, 1984: Temporal variations of the tropical 40-50 day oscillation. Mon. Wea. Rev., 112, 2431-2438.

Anderson, J.R. and D.E. Stevens, 1985: The response of the tropical atmosphere to low Frequency thermal forcing. Submitted to J. Atmos. Sci., April 1985.

Bates, J.R., 1977: Dynamics of stationary ultra-long waves in middle latitudes. Quart. J. Roy. Meteor. Soc., 103, 397-430.

Berkofsky, L., and E.A. Bertoni, 1955: Mean topographic charts for the entire earth. Bull. Amer. Meteor. Soc., 36, 350-354.

Berlage, H.P., 1966: The southern oscillation and world weather. Meded. Verh., 88, 152 pp.

Bjerknes, J., 1969: Atmospheric teleconnection from the equatorial Pacific. Mon. Wea. Rev., 97, 163-172.

Budyko, M.I., 1969: The effect of solar radiation variations on the climate of the earth. Tellus, 21, 611-619.

Chang, C.P., 1977: Viscous internal gravity waves and low-frequency oscillations in the tropics. J. Atmos. Sci., 38, 2254-2364.

Charney, J.G., 1959: On the theory of the general circulation of the atmosphere. The Atmosphere and the Sea in Motion, The Rockefeller Institute Press, 135-162.

Chervin, R.M., and S.H. Schneider, 1976: A study of the response of NCAR GCM climatological statistics to random perturbations: Estimating noise levels. J. Atmos. Sci., 33, 391-404.

Chervin, R.M., and W.H. Washington and S.H. Schneider, 1976: Testing the statistical significance of the response of the NCAR general circulation model to North Pacific Ocean surface temperature anomalies. J. Atmos. Sci., 33, 413-423.

Chervin, R.M., J.E. Kutzbach, D.D. Houghton and R.G. Gallimore, 1980: Response of the NCAR general circulation model to prescribed changes in ocean surface temperature. Part II: Midlatitude and subtropical changes. J. Atmos. Sci., 37, 308-404.

Corby, G.A., A. Gilchrist and P.R. Rowntree, 1977: United Kingdom Meteorological office five-level general circulation model. Methods Comput. Phys., 17, 67-110.

Crutcher, H.L., and J.M. Meserve, 1970: Selected level heights, temperatures and dew points for the Northern Hemisphere, NAVAIR 50-IC-52 Rev., Naval Weather Service Command, Washington, D.C., 8 pp., 408 maps.

Deardorff, J.W., 1978: Efficient prediction of ground surface temperature and moisture, with inclusion of a layer of vegetation. J. Geophys. Res., 83, 1889-1903.

Egger, J., 1977: On the linear theory of the atmospheric response to sea surface temperature anomalies. J. Atmos. Sci., 34, 603-614.

Fennessy, M.J., L. Marx, and J. Shukla, 1985: General circulation model sensitivity to 1982-83 equatorial Pacific sea surface temperature anomalies. Mon. Wea. Rev., 113, 858-864.

Frederiksen, J.S., and B.L. Sawford, 1981: Topographic waves in nonlinear and linear spherical barotropic models. J. Atmos. Sci., 38, 69-86.

Geisler, J.E. and D.E. Stevens, 1982: On the vertical structure of damped steady circulation in the tropics. Quart. J. R. Met. Soc., 108, 87-93.

Gill, A.E., 1980: Some simple solutions for heat induced tropical circulations, Quart. J. Roy. Meteor. Soc., 106, 447-462.

Goswami, B.N., J. Shukla, E.K. Schneider, and Y.C. Sud, 1984: Study of the dynamics of the Intertropical Convergence Zone with a symmetric version of the GLAS climate model. J. Atmos. Sci., 41, 5-19.

Goswami, B.N., and J. Shukla, 1984: Quasi-periodic oscillations in a symmetric general circulation model. J. Atmos. Sci., 41, 20-37.

Hanna, A.F., 1982: Short-term climatic fluctuations forced by thermal anomalies. Atmos. Sci. Paper No. 360, 208 pp.; Department of Atmospheric Science, Colorado State University, Fort Collins, CO 80523 .

Held, I.M., and M. Suarez, 1978: A two level primitive equation atmospheric model designed for climate sensitivity experiments. J. Atmos. Sci., 35, 206-228.

Hendon, H.H., and D.L. Hartmann, 1982: Stationary waves on a sphere: Sensitivity to thermal feedback. J. Atmos. Sci., 39, 1906-1920.

Horel, J.D., and J.M. Wallace, 1981: Planetary-scale atmospheric phenomena associated with the Southern Oscillation. Mon. Wea. Rev., 109, 813-829.

Hoskins, B.J., and D.J. Karoly, 1981: The steady linear response of a spherical atmosphere to thermal and orographic forcing. J. Atmos. Sci., 38, 1179-1196.

Julian, P.R. and R.A. Madden, 1981: Comments on a paper by T. Yasumari. J. Meteor. Soc. Japan, 59, 435-437.

Kasahara, A., and W.M. Washington, 1971: General circulation experiments with a six-year NCAR model, including orography, cloudiness and surface temperature calculations. J. Atmos. Sci., 28, 657-701.

Keshavamurty, R.N., 1982: Respnse of the atmosphere to sea surface temperature anomalies over the equatorial Pacific and the teleconnections of the Southern Oscillation. J. Atmos. Sci., 39, 1241-1259.

Kikuchi, Y., 1969: Numerical simulation of the blocking process. J. Meteor. Soc. Japan, 47, 29-54.

Kubota, I., 1972: Calculation of seasonal variation in the lower tropospheric temperature with heat budget equations. J. Meteor. Soc. Japan, 50, 18-35.

Langley, R.B., R.W. King, I.I. Shapiro, R.D. Rosen, and D.A. Salstein, 1981: Atmospheric angular momentum and the length of day: a common fluctuation with a period near 50 days. Nature, 294, 730-732.

Lorenz, E., 1961: Simplified dynamic equations applied to the rotating-basin experiments. J. Atmos. Sci., 19, 39-51.

Madden, R.A. and P.R. Julian, 1971: Detection of a 40-50 day oscillation in the zonal wind in the tropical Pacific. J. Atmos. Sci., 28, 702-708.

Madden, R.A. and P.R. Julian, 1972: Description of global-scale circulation cells in the tropics with a 40-50 day period. J. Atmos. Sci., 29, 1109-1123.

Manabe, S., J. Smagorinsky and R.F. Stickler, 1965: Simulated climatology of a general circulation model with a hydrologic cycle. Mon. Wea. Rev., 93, 769-798.

Matsuno, T., 1966: Quasi-geostrophic motions in the equatorial area. J. Meteor. Soc. Japan, 44, 24-42.

Murakami, T., T. Nakazawa, and J. He, 1983: 40-50 day oscillations during the northern hemisphere summer. University of Hawaii Meteorological publication UHMET 83-02.

Namias, J., 1976: Negative ocean-air feedback systems over the North Pacific in the transition from warm to cold seasons. Mon. Wea. Rev., 104, 1107-1121.

Otto-Bliesner, B.L., G.W. Branstator and D.D. Houghton, 1982: A global low-order spectral general circulation model. Part I: formulation and seasonal climatology. J. Atmos. Sci., 39, 929-948.

Parker, D.E., 1973: Equatorial Kelvin waves at 100 millibars. Quart. J. Roy. Meteor. Soc., 99, 116-129.

Phillips, N.A., 1956: The general circulation of the atmosphere: A numerical experiment. Quart. J. Roy. Meteor. Soc., 82, 123-164.

Ramage, C.S., 1975: Preliminary discussion of the 1972-73 El Niño. Bull. Amer. Meteor. Soc., 56, 234-242.

Reiter, E.R., 1978: Long-term wind variability in the tropical Pacific, its possible causes and effects. Mon. Wea. Rev., 106, 324-330.

Reiter, E.R., 1979: Trade-wind variability, southern oscillation, and quasi-biennial oscillation. Arch. Meteor. Geophys. Bioklim., A28, 113-126.

Reiter, E.R. and D.R. Westhoff, 1981: Atlas of linear trends in northern-hemisphere tropospheric geopotential height and temperature patterns. Environmental Research Paper 34, 16 pp; Colorado State University, Fort Collins, CO.

Reiter, E.R., 1983: Teleconnections with tropical precipitation surges. J. Atmos. Sci., 40, 1631-1647.

Roads, J.O., and R.C.J. Somerville, 1982: Predictability of ultralong waves in global and hemispheric quasi-geostrophic barotropic models. J. Atmos. Sci., 39, 745-755.

Rowntree, P.R., 1972: The influence of tropical East Pacific Ocean temperatures on the atmosphere. Quart. J. Roy. Meteor. Soc., 98, 290-321.

Rowntree, P.R., 1976: Tropical forcing of atmospheric motions in a numerical model. Quart. J. Roy. Meteor. Soc., 102, 583-605.

Salmon, R., and M.C. Hendershott, 1976: Large scale air-sea interactions with a simple general circulation model. Tellus, 18, 228-242.

Sankar-Rao, M., and B. Saltzman, 1969: On a steady theory of global monsoons. Tellus, 21, 308-330.

Sellers, W.D., 1973: A new global climate model. J. Appl. Meteor., 12, 241-254.

Shukla, J., and J.M. Wallace, 1983: Numerical simulation of the atmospheric response to equatorial Pacific sea surface temperature anomalies. J. Atmos. Sci., 40, 1613-1630.

Stevens, D.E., R.S. Lindzen, and L.J. Shapiro, 1977: A new model of tropical waves incorporating momentum mixing by cumulus convection. Dyn. Atm. Oceans, 1, 365-425.

Stevens, D.E., and R.S. Lindzen, 1978: Tropical wave-CISK with a moisture budget and cumulus friction. J. Atmos. Sci., 35, 940-961.

Stevens, D.E., and G.H. White, 1979: Comments on "Viscous internal gravity waves and low-frequency oscillations in the tropics". J. Atmos. Sci., 36, 545-546.

Thompson, S.L., and S.G. Warren, 1982: Parameterization of outgoing infrared radiation derived from detailed radiative calculations. J. Atmos. Sci., 39, 2667-2680.

Trenberth, K.E., 1976: Spatial and temporal variations of the Southern Oscillation. Quart. J. Roy. Meteor. Soc., 102, 639-653.

Troup, A.F., 1965: The Southern Oscillation. Quart. J. Roy. Meteor. Soc., 98, 490-506.

Walker, G.T., and E.W. Bliss, 1932: World weather V. Mem. Roy. Meteor. Soc., 4, 53-84.

Weare, B.C., A.R. Navato and R.W. Newell, 1976: Empirical orthogonal analysis of Pacific sea surface temperatures. J. Phys. Ocenogr., 6, 671-678.

Webster, P.J., 1983: Mechanisms of low-frequency variability: Surface hydrological effects. J. Atmos. Sci., 40, 2110-2124.

Weickman, K.M., 1983: Intraseasonal circulation and outgoing longwave radiation modes during northern hemisphere winter. Mon. Wea. Rev., 111, 1838-1858.

Wetherald, R.T., and S. Manabe, 1972: Response of the joint ocean-atmospheric model to the seasonal variation of the solar radiation. Mon. Wea. Rev., 100, 42-59.

Yamagata, and Hayashi, 1984: A simple diagnostic model for the 30-50 day oscillation in the tropics. unpublished manuscript.

Yasunari, T., 1980: A quasi-stationary appearance of 30 to 40 day period in the cloudiness fluctuations during the summer monsoon over India. J. Meteor. Soc. Japan, 58, 225-229.

7. Publications

The following publications have resulted from the present NASA Grant:

1. Anderson, John R., 1984: Slow Motions in the Tropical Troposphere, Atmospheric Science Paper No. 381, 143 pp., Colorado State University, Fort Collins, CO 80523.

2. Anderson, John R., 1984a: Low frequency modes of the tropical troposphere. 15th Conference on Hurricanes and Tropical Meteorology (American Meteorological Society), Jan. 9-13, 1984, Miami, Florida. Pre-print volume, pp. 509-511.

3. Anderson, J.R., and D.E. Stevens, 1985: The response of the tropical atmosphere to low frequency thermal forcing. Submitted to J. Atmos. Sci., April 1985.

4. Anderson, J.R., D.E. Stevens, and P.R. Julian, 1984: Temporal variations of the tropical 40-50 day oscillation. Mon. Wea. Rev., 112, 2431-2438.

5. Geisler, J.E. and D.E. Stevens, 1982: On the vertical structure of damped steady circulation in the tropics. Quart. J. R. Met. Soc., 108, 87-93.

6. Hanna, A.F., 1982: Short-term climatic fluctuations forced by thermal anomalies. Atmospheric Science Paper No. 360, 208 pp, Colorado State University, Fort Collins, CO 80523.

7. Hanna, A.F., E.R. Reiter, and D.E. Stevens, 1983: Short-term climatic fluctuations forced by thermal anomalies. Paper prepared for the First International Conference on Southern Hemisphere Meteorology; July 31-August 6, 1983; Sao Jose Dos Campos, Brazil.

8. Hanna, A.F., D.E. Stevens and E.R. Reiter, 1984: Short-term climatic fluctuations forced by thermal anomalies. J. Atmos. Sci., 41, 122-141.

9. Hanna, A.F. and D.E. Stevens, 1984: A global low order spectral model designed for climate sensitivity studies. Atmospheric Science Paper No. 378, 49 pp., Colorado State University, Fort Collins, CO 80523.

10. Reiter, E.R. and D.R. Westhoff, 1981: Atlas of linear trends in northern-hemisphere tropospheric geopotential height and temperature patterns. Environmental Research Paper 34, 16 pp., Colorado State University, Fort Collins, CO 80523

11. Stevens, D.E., and A.F. Hanna, 1983: The general circulation of a simple, two-level model atmosphere. IAMAP-WMO Symposium on Maintenance of the Quasi-stationary components of the Flow in the Atmosphere and in Atmospheric Models. Paris, Aug. 29 - Sept. 2, 1983. Extended Abstracts Volume, p. 287.

Notes:

Dr. John Anderson was awarded the Max Eaton prize of American Meteorological Society for his presentation of paper #2 in the publication list.

A manuscript describing the free mode calculations of Section 5.2 is currently in preparation for submission to a journal.

The papers listed in the publication list are included as attachments 1 through 11 to this report.